Review article **Open Access**

En Cao[a], Weihua Lin[a], Mengtao Sun*, Wenjie Liang* and Yuzhi Song*

Exciton-plasmon coupling interactions: from principle to applications

DOI 10.1515/nanoph-2017-0059
Received May 25, 2017; revised June 14, 2017; accepted June 21, 2017

Abstract: The interaction of exciton-plasmon coupling and the conversion of exciton-plasmon-photon have been widely investigated experimentally and theoretically. In this review, we introduce the exciton-plasmon interaction from basic principle to applications. There are two kinds of exciton-plasmon coupling, which demonstrate different optical properties. The strong exciton-plasmon coupling results in two new mixed states of light and matter separated energetically by a Rabi splitting that exhibits a characteristic anticrossing behavior of the exciton-LSP energy tuning. Compared to strong coupling, such as surface-enhanced Raman scattering, surface plasmon (SP)-enhanced absorption, enhanced fluorescence, or fluorescence quenching, there is no perturbation between wave functions; the interaction here is called the weak coupling. SP resonance (SPR) arises from the collective oscillation induced by the electromagnetic field of light and can be used for investigating the interaction between light and matter beyond the diffraction limit. The study on the interaction between SPR and exaction has drawn wide attention since its discovery not only due to its contribution in deepening and broadening the understanding of SPR but also its contribution to its application in light-emitting diodes, solar cells, low threshold laser, biomedical detection, quantum information processing, and so on.

Keywords: exciton; plasmon; coupling interactions; principle; application.

[a]**En Cao and Weihua Lin:** These authors contributed equally to this work.

***Corresponding authors: Mengtao Sun,** Department of Physics, Shandong Normal University, Jinan, Shandong, People's Republic of China; Beijing Key Laboratory for Magneto-Photoelectrical Composite and Interface Science, Center for Green innovation, School of Mathematics and Physics, University of Science and Technology Beijing, Beijing 100083, People's Republic of China, e-mail: mengtaosun@ustb.edu.cn. http://orcid.org/0000-0002-8153-2679; and Beijing National Laboratory for Condensed Matter Physics, Beijing Key Laboratory for Nanomaterials and Nanodevices, Institute of Physics, Chinese Academy of Sciences, Beijing 100190, People's Republic of China; **Wenjie Liang,** Beijing National Laboratory for Condensed Matter Physics, Beijing Key Laboratory for Nanomaterials and Nanodevices, Institute of Physics, Chinese Academy of Sciences, Beijing 100190, People's Republic of China, e-mail: wjliang@iphy.ac.cn; and **Yuzhi Song,** Department of Physics, Shandong Normal University, Jinan, Shandong, People's Republic of China, e-mail: yzsong@sdnu.edu.cn

En Cao: Department of Physics, Shandong Normal University, Jinan, Shandong, People's Republic of China; and Beijing National Laboratory for Condensed Matter Physics, Beijing Key Laboratory for Nanomaterials and Nanodevices, Institute of Physics, Chinese Academy of Sciences, Beijing, People's Republic of China

Weihua Lin: Beijing Key Laboratory for Magneto-Photoelectrical Composite and Interface Science, School of Mathematics and Physics, University of Science and Technology Beijing, Beijing, People's Republic of China; and Beijing National Laboratory for Condensed Matter Physics, Beijing Key Laboratory for Nanomaterials and Nanodevices, Institute of Physics, Chinese Academy of Sciences, Beijing, People's Republic of China

1 Introduction

Frenkel first proposed the concept of excitons in 1931 [1]. An exciton (an electrically neutral quasi-particle) is a bound state of an electron and a hole, which are attracted to each other by the electrostatic Coulomb force. The exciton exists in semiconductors, insulators, and some liquids, which can transfer energy without transporting net electric charge [2, 3]. The decay of the exciton is limited by resonance stabilization because of the overlap of the hole and electron wave functions, which results in the lifetime of the exciton being extended.

Surface plasmons (SPs) are the collective oscillations of free electrons that are confined evanescently on a metal surface [4]. There are two kinds of SPs, which called localized SPs (LSPs) and propagating SPs (PSPs; or plasmonic waveguide) [5, 6]. LSPs are oscillations of charge density that are confined on the surface of a metallic nanoparticle. The resonant LSPs, known as LSP resonance (LSPR), result in a large enhancement of the localized electromagnetic (EM) field, which is the underlying mechanism for surface-enhanced spectroscopy [7]. SPs, coupled with photons, can act as a collective excitation of conduction

electrons that propagate in a wave-like manner along an interface between a metal and a dielectric, known as SP polaritons (SPPs). SPPs are confined to the vicinity of the interface and can propagate along the metal surface until the energy dissipates either by heat loss or by radiation into free space [8].

The interaction of exciton-plasmon coupling and the conversion of exciton-plasmon-photon have been widely investigated experimentally and theoretically [9–31]. SP modes can coherently hybridize with molecular excitons, and its large oscillator strength can lead to a so-called strong coupling regime. In a strong exciton-plasmon coupling regime, a coherent coupling between LSPs and excitons overwhelms all losses and results in two new mixed states of light. Hence, matter is separated energetically by a Rabi splitting that exhibits a characteristic anticrossing behavior of the exciton-LSP energy tuning [32–34]. In this regime, a new quasi-particle (plexciton) forms with distinct properties possessed by neither original particle. In the weak coupling regime, the resonant molecules can be treated as dielectric materials with a complex refractive index (RI) in dispersion. Through the Kramers-Kronig relations, the wavelength dependence of the real part of the RI is related to the molecular absorption resonance as described by the imaginary part of the RI [35]. As a result, switching the molecular resonance can change the real part of the RI and thus cause LSPR peak shifts due to the sensitivity of the LSPR to the RI of the surroundings [36, 37].

These investigations can not only reveal the nature of light-matter interaction but also promote the applications of exciton-plasmon hybrids in the field of energy, catalysis, environment, and optical communications. In this review, we first introduce the basic principle of exciton and plasmon and then review recent progress of the applications of exciton-plasmon interaction in different fields.

As we know, when the incident light illuminates the metal surface of conductor, it will cause the surface collective oscillation of free electrons, which is the so-called LSPs or LSPR. The frequency of LSPR (ω_L), also the frequency of free electrons on the surface of metallic (such as silver and gold) nanoparticles, can be well controlled by tuning the sharp size of nanoparticles and changing the surrounding dielectric medium [38–40]. At the resonance condition, incident photon energy can be efficiently confined into small area by LSP mode, which can also enhance the local EM fields [41]. Strong EM fields can also be monitored under the influence of the properties of light-matter interaction in systems, quantum-confined nanostructures [42, 43], and other excitonic systems.

2 Basics of the physics

2.1 Brief introduction to SPs

SP has aroused much attention since its discovery. The appearance of SPs is due to the collective oscillation of free electrons between the metal and dielectric media. When the incident light with a fixed wavelength is irradiated to the surface of the metal, it can result into enormous enhancements of SPR [44] and localized field of EM on the surface of the metal. In addition, it is widely applied in surface-enhanced Raman scattering (SERS) and tip-enhanced Raman scattering (TERS) [45, 46]. Generally, SPs can be divided into LSPs and PSPs, and both their schematic diagrams are shown in Figure 1. In view of the unique properties of SP, it plays a key role in the spectrum of science ranging from physics to biology [48].

2.2 Brief introduction to surface exciton

The surface of solid that is illuminated by a beam of incident light will produce a bound pair of electron hole due to the absorption of photons [49, 50]. In the meantime, the electrons of the conduction band and the holes of the valence band form a new bound state due to the Coulomb interaction, which is often called exciton.

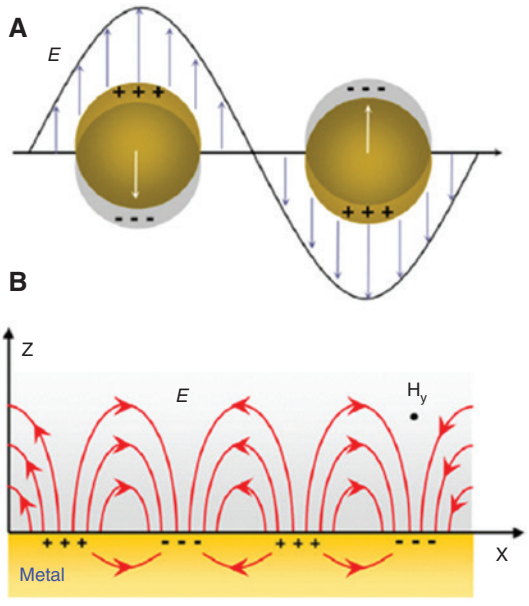

Figure 1: Sketches of the mechanism of LSPs, PSPs. (A) LSPs are collective oscillation of free electrons confined on the surface of metal nanoparticles and (B) PSPs are excitation of collective electrons that can only propagate near the vicinity of the interface [47].

Normally excitons are divided into two categories, named Wanner [51] and Frenkel [52] exciton, respectively. The former is mainly present in semiconductor materials, which has the similar characteristics of weak Coulomb interaction and wide distribution of electrons and holes. The latter is generally present in insulating materials, which has the characteristics of strong Coulomb interaction, and the electrons are bound in somatic cells as well as the holes.

This field has attracted the attention of researchers and a series of studies have been carried out [50, 53–55]. Excitons are well suited to describe the optical properties of semiconductors. Because the bound energy of excitons is very high, the free excitons are more easily to be bound to the impurity; hence, the luminescent center formed. Simultaneously, the excitation effect has a significant influence on luminous, light absorption, and optical nonlinear effects in semiconductors [56, 57]. This finding paves the way to the development and advanced research of semiconductor optoelectronic devices.

2.3 Brief introduction to the interaction between LSPs and excitons

When the resonant frequency of the SP is very close to the frequency of the molecular energy level, the exchange energy between LSPs and excitons becomes an important factor affecting their interaction. At this point, the interaction between LSPs and excitons has not been explained by the dielectric function. Moreover, according to whether there is perturbation between wave functions, the coupling between LSPs and excitons can be divided into strong coupling and weak coupling [58]. When the molecule and the SP are coupled into a hybrid state, there is a perturbation between wave functions. The resonance exchange energy occurs between the upper and lower levels of the newly formed hybrid state (also called Rabi oscillation), which can be described as strong coupling. The strong coupling phenomenon can be proven by Rabi splitting in the stability spectrum [59] and the anticrossing phenomenon of the energy corresponding to the splitting peak at different coupling intensities [60]. When we talk about using SPs to promote absorption [61], SERS effects [62], fluorescence [63], and fluorescence quenching [64], the interaction that has no perturbation between wave functions can be called as weak coupling.

The interaction between LSPs and excitons in semiconductor nanostructures can achieve their complementary advantages on optical performance, such that the lifetime of excitons is prolonged in semiconductor nanostructures as well as the yield of quantum is greatly increased [65, 66]. Metal nanostructures can produce the energy of localized EM field and enhance the intensity of electric field [67] and the nonlinear effect [68]. In view of the superior nature of these two materials, it is proposed that these two materials can be combined in a systematic manner. Therefore, we can achieve a composite structure with specific optical properties and can observe the new phenomenon of the interaction between SPs and excitons [69–72].

3 Strong exciton-plasmon coupling

The strong coupling of exciton-plasmon is achieved when the energy that transfers between the light and exciton is larger than their average dissipation, with the formation of a matter-light hybrid state and a new quasi-particle (plexciton) with distinct properties possessed by neither original particle [73]. In strong coupling regime, the new model, which has different properties of the two resonators involved (the resonators are photons and excitons, respectively, where we assume in the semiconductor resonator), results in a series of interesting phenomenon and shows great value in different areas of application [74]. A new polaron is formed by the interaction between light and excitons, and the formation may also lead to the Bose-Einstein condensation [75]. In the field of quantum information, strong coupling can achieve quantum coherent oscillation, which plays a key role in quantum information processing [76]. Moreover, the EM environment of fluorophore can be changed by strong coupling [77], so it can be used to change the threshold of the chemical reaction and control the rate of chemical reactions. The strong coupling of superconducting quantum bits and microwave can be applied to routers [78], photon detectors [79], and single-photon switches [80].

Generally, we introduce the interaction between light and matter as exciton-plasmon coupling in the microcavity environment. Strong coupling is defined by the following three important parameters [81]: g = energy transfer rate between light and matter, κ = rate of light escape from the cavity, and γ = rate of matter loses its polarization.

When the rate of the energy transfer between light and matter is faster than the other two rates, there will be a strong coupling. The energy exchange between light and matter will be periodical. At rate g when the matter and microcavity will resonate, the two new resonance frequencies can be observed from reflectance and transmittance spectrum (see Figure 2). The form of the resonant frequency can be expressed as

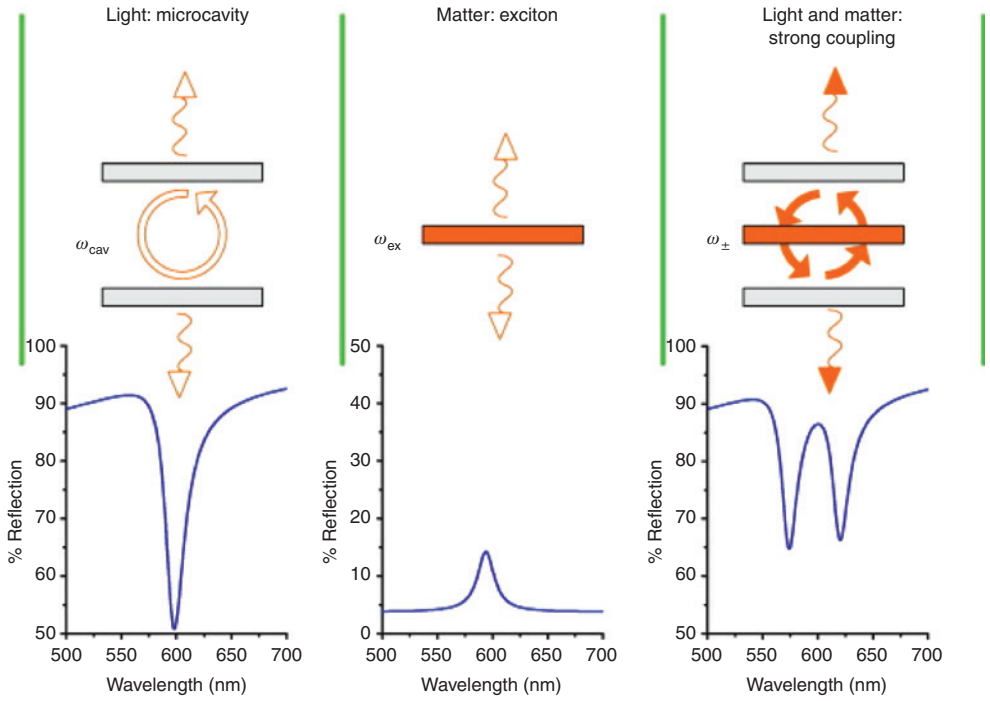

Figure 2: Sketch of the reflectance spectra showing the results of the strong coupling of light and matter.
The microcavity (light) and matter (exciton layer) are provided with resonant frequencies of X_L and X_M. When strong coupling arises, the integrated system represents new resonances at X_{-}^{+} [82].

$$\omega_{\text{exciton}} = \omega_{\text{cavity}} = \omega_0 \pm g \text{ (new frequency)}.$$

In strong coupling regime, the appearance of anticrossing dispersion is also called Rabi splitting [74]. First of all, we need to understand the Rabi oscillations.

3.1 Rabi oscillations

Generally speaking, when the laser illuminates the materials, there is a fluctuation of population between levels, of which the oscillation frequency is the Rabi frequency. The pulse time, which is less than the relaxation time of the medium, must be met and consider the damping to understand that the particle in the excited state of lifetime is greater than the time of pulse.

Many of the excitation of the electron systems can be well described by the liner response scheme, and the nonlinear interaction between light and matter is recognized as the origin of many physical processes [83]. Rabi oscillations, which occur between stationary states of systems of two-state quantum near an oscillatory driving fields and its energy transitions, are periodical. The form of the field can be written as

$$E(t) = E_0 \cos(\omega t) \tag{1}$$

With frequency close to the frequency of resonance $|\omega - \omega_0| \ll \omega_0$.

The interaction of Hamiltonian can well describe the interaction of atomic fields, where the form between the field and the atom can be written as

$$\hat{H}^I(t) = \hat{d} \cdot E(t) = -\hat{d}\cos(\omega t) \tag{2}$$

where $\hat{d}$ is the operator of dipole moment. The form of total Hamiltonian of interaction of the atomic field system can be written as

$$\hat{H} = \hat{H}_{\text{atom}} + \hat{H}_{\text{field}} + \hat{H}^I(t) \tag{3}$$

where $\hat{H}_{\text{atom}}$ is the Hamiltonian of free atoms, which can be written as

$$\hat{H}_{\text{atom}} = \frac{1}{2}\hbar\omega_{eg}(|e\rangle\langle e| - |g\rangle\langle g|) \tag{4}$$

If we ignore the effects of quantum fields, Equation (3) can be changed into

$$\hat{H} = \hat{H}_{\text{atom}} + \hat{H}^I(t) \tag{5}$$

Combining Equations (2) and (4), we can obtain the final form of $\hat{H}$

$$\hat{H} = \hbar\omega_{eg}|e\rangle\langle e| - \hat{d}\cos(\omega t) \tag{6}$$

The system state vector is

$$|\Psi(t)\rangle = \sum_k c_k(t) e^{\frac{-iE_k t}{\hbar}} |k\rangle = c_g(t)|g\rangle + c_e(t) e^{-i\omega_{eg} t} |e\rangle \quad (7)$$

Substituting Equation (7) into the time-dependent Schrödinger equation,

$$i\hbar \frac{\partial |\Psi(t)\rangle}{\partial t} = \hat{H} |\Psi(t)\rangle \quad (8)$$

Combining Equations (7) and (8), the amplitudes of coupled first-order differential equations are obtain as

$$\dot{C}_e = -\frac{i}{h} E_0 \cos(\omega t) d_{eg}^* e^{-i\omega_{eg} t} C_g \quad (9)$$

$$\dot{C}_g = -\frac{i}{h} E_0 \cos(\omega t) d_{eg} e^{i\omega_{eg} t} C_e \quad (10)$$

After expanding $\cos(\omega t)$ and applying the rotating wave approximation (RWA), which means neglecting the quickly rotating terms, as the time evolution induced by the applied field is much slower than ω_0, one obtains (introducing the detuning, $\Delta = \omega_{eg} = -\omega$)

$$\dot{C}_e = -\frac{i}{2\hbar} E_0 d_{eg}^* e^{-i\Delta t} C_g \quad (11)$$

$$\dot{C}_g = 0 \quad (12)$$

Equation (2) is integrated to

$$C_e = -\frac{i d_{eg}^* E_0}{\hbar} e^{\frac{i\Delta t}{2}} \sin\left(\frac{\Omega_R t}{2}\right) \quad (13)$$

$$\Omega_R = \sqrt{\Delta^2 + \frac{(i d_{eg}^* E_0)^2}{\hbar^2}} \quad (14)$$

Of which, Ω_R is the frequency of Rabi and Δ is the Rabi splitting energy.

3.2 Rabi splitting

The strong coupling regime has caused a lot of attention. Thus far, the fields of research have focused on two major areas: solid physics (mostly semiconductor) and atomic physics. The former studies concentrated on the modified photonic gap in 3D structure [84] and spontaneous emission [85, 86]; the latter majors in the interaction of atom cavity [87].

In this review, we present an effect of solid-state quantum electrodynamics (QED) and a system of atom cavity can be created by placing the atoms into the optical microcavity. The splitting has been observed from both the atomic fluorescence spectrum [88] and the transmission resonances of empty cavity [89]. Simultaneously, the phenomenon of splitting called vacuum Rabi splitting (VRS) is used to describe the quantum properties of EM fields [90].

First of all, Rabi splitting must be understood when we want to study quantum cavity electrodynamics.

3.2.1 Quantum cavity electrodynamics

QED shows that the spontaneous emission of atoms is the process of interaction between atoms in vacuum fields. There are various EM coupling between atoms in free space, of which the spontaneous emissivity is irreversible [91]. Until 1995, Purcell [92] found that the spontaneous emissivity of the moment of magnetic in the resonant circuit increases compared to the free space. In the atom cavity system, the geometric length of the cavity can adjust the model of EM field density, affecting the cavity of the atomic EM coupling as well as changing the spontaneous emissivity of the atom. Through Milonni and Knight's [93] further calculation, when half the wavelength of the spontaneous emission of atoms is larger than the length of the cavity, the spontaneous emission of the cavity atoms parallel to the transition dipole moment will be suppressed. In 1985, Hulet et al. [94] first discovered the role of cavity on atomic suppression. They placed a Rydberg atom in the high-quality cavity and successfully detected that the atomic energy in the cavity of the excitation life is 20 times in vacuum.

Recently, the coupling between the atoms in the cavity and the EM field becomes an important aspect of QED. In the experiment, the dielectric cavity not only can provide a specific mode of EM field but also can affect the distribution of the vacuum field, and the behavior can be attributed to cavity-QEDs [95, 96]. In this cavity-QED system, the two quantum resonator systems that are coupled to each other can be seen as consisting of atoms and cavities, and the interaction between atomic and quantum single-mode EM exists as a continuous energy exchange. Hence, the state of the whole system is in the superposition of the two subsystems (coherent state). Of course, the continuous exchange of energy is an ideal phenomenon; indeed, the recent improved quantum system is still not completely isolated from the outside world.

The coherent system that we have discussed is made up of the external environment and the cavity-QED system. As we all know, there is an interaction that exists between the system and the external environment, which will make them entangled [97]. If we ignore the external environment system, the entanglement will lead to a decreased coherence of the system itself, which is also named as the decoherent mechanism [98]. The existence of the decoherent mechanism can make the energy exchange between the atoms and the magnetic field weaker until it disappears. Nowadays, researchers seek a variety of ways to reduce the influence of cavity EM such as reducing the volume [99], coating [100], and superconductivity of cavity [101] to increase the coherence interaction intensity. When this coherent mechanism is dominated rather than the decoherent mechanism, we usually called it the strong coupling.

3.2.2 Strong coupling conditions of cavity-QED

The J-C model can well describe the interaction between atoms and cavities in the ideal cavity-QED system (ignore the existence of coherent mechanism), which can be written as [102]

$$\hat{H} = \frac{1}{2}\hbar[(\omega_1\hat{\sigma}_1 + \omega_0) + \omega_1\hat{a}\hat{a}^+ + g(\hat{a}\hat{\sigma}_+ + \hat{a}^+\hat{\sigma})] \tag{15}$$

where $\hat{a}$ and $\hat{a}^+$ are annihilation and generation, respectively. ω_1 and ω_0 are the atomic transition frequency and resonant frequency of the cavity. $\hat{\sigma}_1$, $\hat{\sigma}$, and $\hat{\sigma}_+$ are the inversion, derating, and ascending of atoms. $g(R)$ is the coefficient of coupling between atoms and cavities, which can be written as

$$g(R) = g_0\Psi(R) \tag{16}$$

where $\Psi(R)$ is cavity function. g_0 is the maximum coupling coefficient, whose form can be written as

$$g_0 = \left(\frac{\mu^2\omega_0}{2\hbar\varepsilon_0 V}\right)^{\frac{1}{2}} \tag{17}$$

where V is the volume of the cavity and μ is the atomic transition dipole moment. Thus, it can be seen from Equation (17) that the coupling of the atomic and EM in the cavity increases when the volume of the cavity decreases.

As shown in Figure 3, κ is the attenuation coefficient of the cavity field. The lifetime of the atom in the cavity is represented by 2κ; however, the main factor affecting

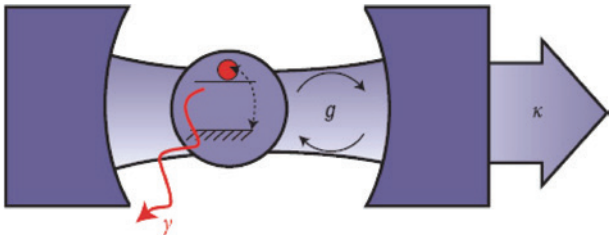

Figure 3: Characteristic parameter diagram of cavity-QED. g is the coupling coefficient of atomic and cavity EM fields. κ is the attenuation coefficient of the cavity field. γ is the dephasing rate for single two-level atom [103].

the life of the photon is the factor of quality (Q) of the cavity, and Q ($Q = \omega_0/2\kappa$) can determine whether the photon in the cavity disappears quickly or slowly due to various losses [104]. γ can be divided into longitudinal attenuation γ_1 and lateral attenuation γ_2. According to the Weisskopf-Wigner theory, there is an interaction that exists between μ and γ_1 (also known as spontaneous emissivity) [105].

$$\gamma_1 = \frac{\mu^2\omega_0^3}{3\pi\varepsilon_0\hbar c^3} \tag{18}$$

where c is the speed of light in free space. The form of Equation (17) can be written as

$$g_0 = \left(\frac{3c\lambda^2\gamma_1}{8\pi V}\right)^{\frac{1}{2}} \tag{19}$$

At present, the optical cavity is widely used in the experiment, γ_2 is the radiation transition; when we ignore the relative position, it can be considered as $\gamma_2 = \gamma = \gamma_1/2$. γ_1 is used to represent the excited state of the atomic transition and the probability of radiating, which is determined by the Einstein spontaneous emission coefficient (A), $\gamma_1 = A$. When the parameters meet $g_0/(\gamma, \kappa) > 1$, the interaction between the cavity field and the atom in the system is dominated by various decoherence mechanisms; hence, the cavity-QED system exists in a strong coupling field.

3.2.3 VRS

The cavity-QED establishes a good cavity coupled with the atomic system, compared to an independent atom or cavity, and the quantum behavior of the coupled system is richer. In 1983, Wu et al. [106] found the splitting in the atomic spectrum VRS by studying the strong coupling

between atoms and cavity. Agarwal [107] proved that VRS can lead to bimodal characteristics of the transmission spectrum of the cavity.

In the past, the research in the field of cavity electrodynamics has focused on the atomic system [108], and new progress has been made through many quantum optics experiments [60, 109]. In cavity-QED, the quantum mechanism by studying the nature of the interaction between light and matter is explained by VRS. Fink et al. reported that quantum nonlinearity is obtained by observing the spectrum, and the atomic-photon superposition state involving up to two photons is explored using spectral pumps and probe techniques.

Jaynes-Cummings Hamiltonian can well describe the dynamics of a system of two-level coupled to an EM, which can be written as [108]

$$H = \hbar\omega_0 \hat{a}^+\hat{a} + \hbar\omega_{ij}\hat{\sigma}_{ij} + \hbar g_{ij}\hat{\sigma}_{ij}^+\hat{a} + \hbar g_{ij}\hat{\sigma}_{ij}\hat{a}^+ \tag{20}$$

where ω_0 is the frequency of the resonator field and $\hat{a}^+$ and $\hat{a}$ are the raising and lowering operators, respectively. ω_{ij} is the frequency of transition between the ground state $|i\rangle$ and excited state $|j\rangle$. g_{ij} is the strength of coupling between the two states. $\sigma_{ij} = |i\rangle\langle j|$ is the corresponding operator. As we all know when $g_{ij}/(\gamma, \kappa) > 1$, the strong coupling is limited. When $\omega_0 = \omega_{ij}$, in the case of n excitons, the coupled system has new eigenstates, which are antisymmetric $(|i, n\rangle - |j, n-1\rangle)/\sqrt{2} \equiv |n+\rangle$ and symmetric $(|i, n\rangle - |j, n-1\rangle/\sqrt{2} \equiv |n-\rangle)$ qubit-photon superposition states, respectively (as shown in Figure 4). At frequency $2g_{ij}$, $n=1$, the VRS of these states can be observed (see Figure 4).

In a strong coupling system, coherent energy exists in an exchange between the cavity mode and the atom when the cavity mode resonates with the atom. The corresponding atomic energy level split, and two nondegenerate eigenmodes appear in the system, which correspond to the VRS of the two edge bands.

4 Application of strong coupling

4.1 Modification of the rate of chemical reactions

Just as the orbital of the molecule is formed by atomic exchange electrons, electron field occurs with the exchange of photons, and because of this behavior, the

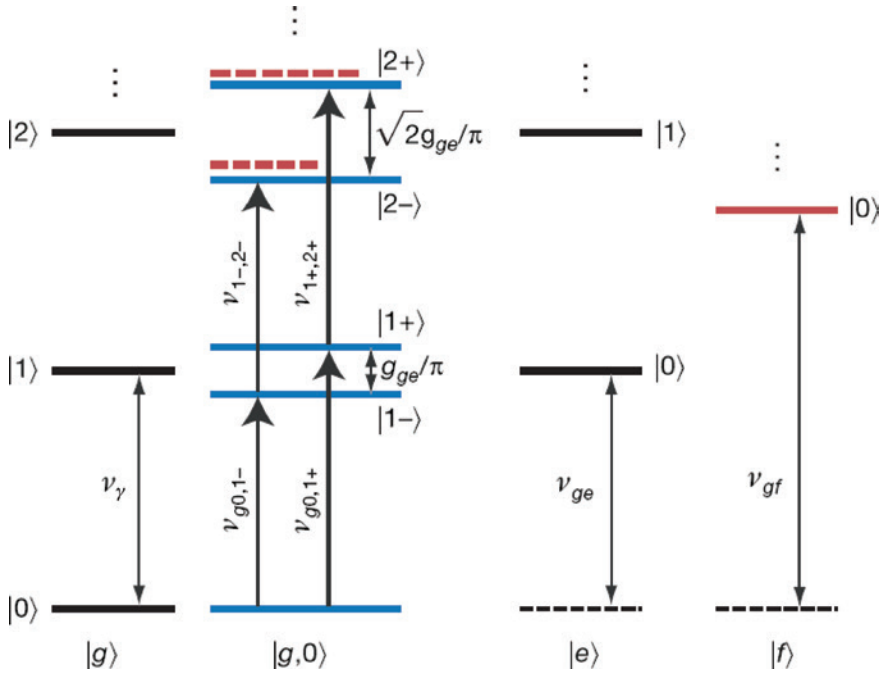

Figure 4: Diagram shows a resonant cavity-QEDs.
$|g\rangle$, $|f\rangle$, and $|e\rangle$ are uncoupled qubit states and $|0\rangle$, $|1\rangle$, and $|2\rangle$ are photon states. ν_γ is the frequency of cavity and ν_{ge} is the frequency of transition between the ground state $|g\rangle$ and the excited state $|e\rangle$. The blue line represents the dipole-coupled dressed states. The energy of all ground states is represented by black lines. Pump and probe transitions are given as ($\nu_{g0,1-}$, $\nu_{g0,1+}$) and ($\nu_{1-,2-}$, $\nu_{1+,2+}$), respectively [108].

EM and quantum system can interact with each other. As mentioned above, when the interaction between the two systems is strong enough to overcome decoherence effects, the new hybrid state will be formed, which is called Rabi splitting (see Figure 5).

The premise of the emergency of strong coupling is that the material must be in the optical cavity. Generally, two parallel mirrors make up the cavity (see Figure 6), which can be tuned to resonance with the excited state.

Coupling to the vacuum field can cause the energy level of the molecule to be rearranged; hence, the reaction rates and yields can be modified. The reorganization of molecular energy levels can determine the role of strong coupling as to slow down or speed up the reaction rate [112]. In the vacuum field, both the thermodynamics and rates of the reaction can be modified. In the vacuum field, the strong coupling of the reaction is obvious, such that the molecule retains its original electronic structure in the reaction and the rate of reaction can be increased by concentrating the light. Although in strong coupling the Rabi splitting and the spectrum shape can be predicted by the semiclassical theory, it cannot be used to predict their interrelationships, dynamics, and discrete states lifetime [113]. Coupling not only acts on the electron transition but also changes the reactivity of the chemical bond. As already mentioned, the strong coupling formed by the hybrid state can change the energy level and in principle can also change the system of electron affinity and ionization potential [114]. It is important to note that strong coupling is not limited to the configuration of Fabry-Perot.

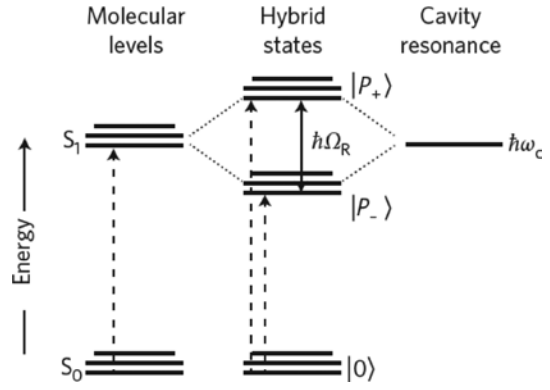

Figure 5: Simplified energy landscape shows that there is an energy exchange between the transition (HOMO-LUMO) of molecules and the cavity, which is rapid compared to energy loss. Two hybrid states ($|P+\rangle$ and $|P-\rangle$) are formed due to strong coupling. Note that the coupled system ground-level energy $|0\rangle$ may be modified by strong coupling [110].

Any structure of photonics provides a resonance of sufficiently sharp characteristic [115].

In summary, the cavity vacuum field for modifying the properties and chemical reactions of molecules puts a new tool into influencing useful reactions, with implications for molecular devices and materials science. Therefore, it has a very great potential for the field of technology, which is worth of further exploration.

4.2 Quantum information processing

The fundamental and revolutionary results of the quantification have not been raised until the first discovery of Shannon in 1948 [116]. Binary digit and bits as information carriers provide a way of how to distinguish information; even if there is noise, information can be faithfully transmitted. Driven by this technology, the information processing speed and computing power achieve exponential growth, as bits continue to be reduced to a single molecule size. At the nanometer scale, the classic Moore's law began to hold sway (the days of Moore's law are numbered) [98]. In the 1980s, Richard Feynman and Paul Benioff proved that the classic bits can still be manipulated and stored. Even if we find a way to reach the limit, there is no room for further gain in the absence of an atomic split.

Information science plays a major role in our lives. However, communication networks, electronic computers, and other electronic equipment have been closed to the information processing limit. Therefore, quantum information was generated and it has an advantage that classic information cannot complete, such as information processing functions. Quantum information needs to be processed in the study of quantum information. At the same time, the hardware is essential; thus far, it has been proposed for the program cavity-QED [97, 117, 118], nuclear magnetic resonance [119, 120], and ion trap [121, 122]. The solution that is considered to be the most promising is cavity-QED [112]. The atoms in the optical cavity are most suitable for quantum information storage. The main idea of cavity-QED has been confined as capturing atoms in high quality and storing the information on the atomic energy state. In the cavity, due to the coupling of atoms and cavity field mode, there is an interaction between atoms, so that we can use this scheme for the preparation of atomic entangled states (see Figure 7) to achieve the transmission of atomic information with the purpose of storage.

Here, we briefly describe how to use the scheme of cavity-QED to prepare atomic entanglement. We assume that the two atoms A and B are in ground state $|i_1\rangle$ and

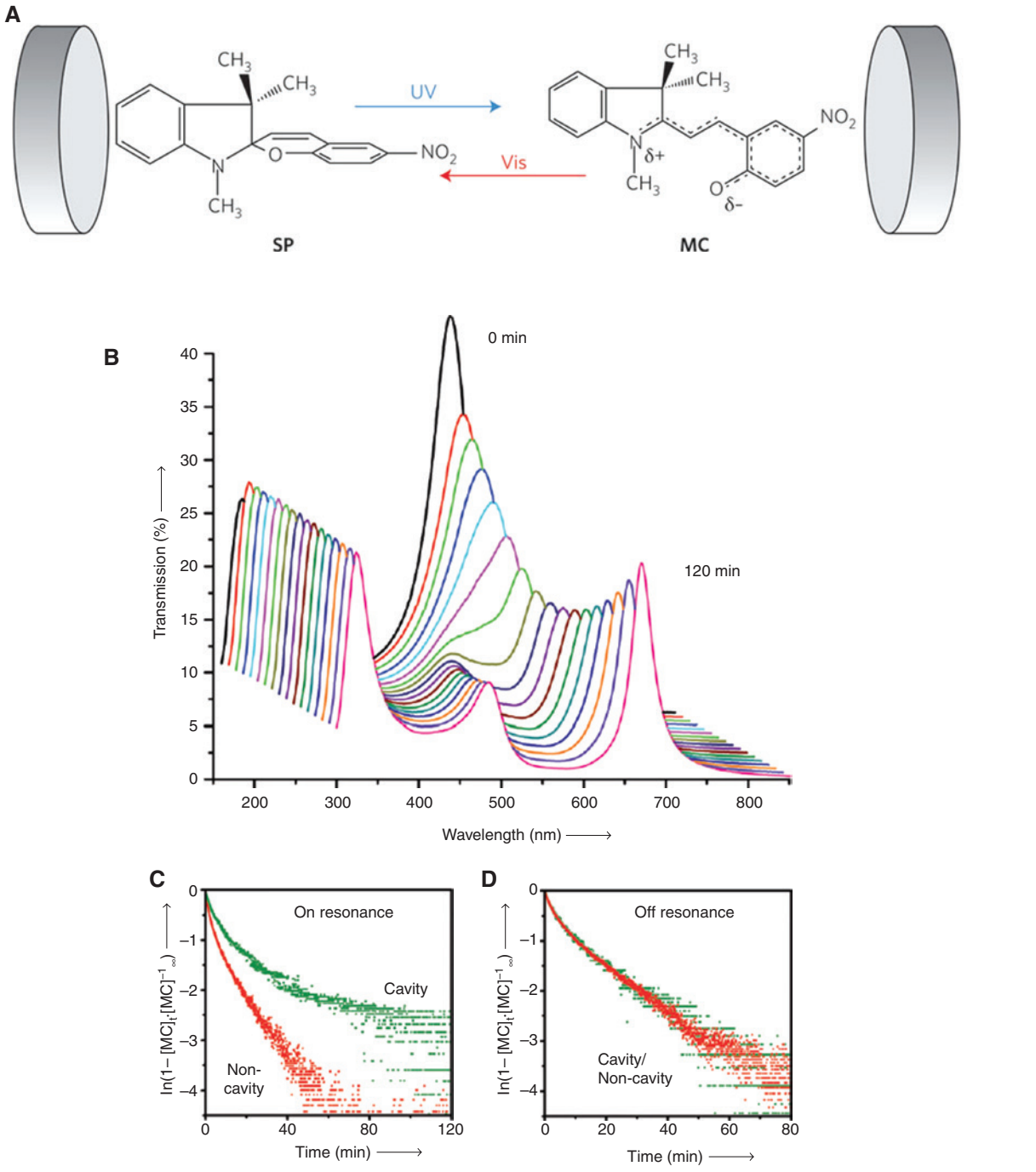

Figure 6: Schematics of the mechanism of phonochromic conversion and related evidence.
(A) Schematic of the conversion of phonochromic between spiropyran (SPI) [44] and merocyanine (MC) in an optical cavity [111]. (B) Spectrum of transmission of the coupled system in the cavity. Noted that the initial mode of Fabry-Perot at 560 nm with the SPI to MC photoreaction proceeds to splitting and two new modes formed. (C) Measurement of the absorbance of MC. The red and green lines represent the uncoupled (bare molecules) and coupled system, respectively. For this case, the resonant frequency of the cavity is tuned to match the absorption frequency of MC at 560 nm, and the difference in the rate of increase of the coupling strength increases gradually. (D) In contrast, the rate of photoisomerization is identical to the sample of noncavity [110].

excited state $|j_2\rangle$, and the cavity is in the vacuum field $|h\rangle$. Put the two atoms into the cavity at the same time, and let the atoms interact with the cavity after time t leaves the cavity. Then, the interaction between two atoms and the cavity field need to be described, and the evolution of the system state can be written as [124]

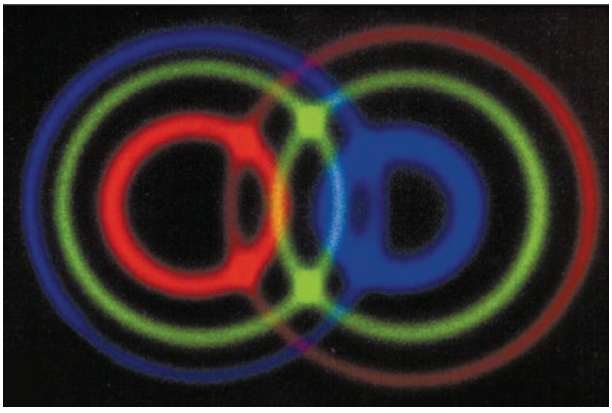

Figure 7: Several cone pairs can be seen along the direction of the optical axis.
The pairs of photon emitted along the cone intersections are entangled in polarization [123].

$$|i_1\rangle|j_2\rangle|h\rangle \rightarrow e^{-i\lambda t}[\cos(\lambda t)|i_1\rangle|j_2\rangle - i\sin(\lambda t)|j_2\rangle|i_1\rangle]|h\rangle \quad (21)$$

From Equation (21), we can see that, when λt is equal to $\pi/4$, we can get two atoms with the largest entangled state that can be written as

$$|\Psi\rangle = |i_1\rangle|j_2\rangle - |j_1\rangle|i_2\rangle/\sqrt{2} \quad (22)$$

Quantum information is an emerging science that uses the unique quantum mechanics of the physical system to store, process, encode, and transmit information [125, 126]. Quantum information shows a lot of novelty, such that one can establish a secure cryptography based on the quantum that cannot be cloned. Through the quantum stacking performance, the operation rate can be rapidly increased. Distributed quantum computing can be achieved by quantum entanglement that can connect different quantum dots. In short, the development of quantum information science for the future development of information technology outlines the intoxicating blueprint.

4.3 Low threshold laser

The spontaneous emission of atoms act differently in microcavity compared to that in the free space. The microcavity can enhance or suppress the spontaneous emission of atoms, so that spontaneous radiation can be a reversible process. The resulting cavity-QED can be used to explain the interaction between atoms with the field of cavity [127]. Here, we introduce an important application – low threshold laser.

In 1917, Einstein discovered the existence of two kinds of excited atoms: spontaneous radiation and stimulated radiation. Since the invention of the laser in 1960, researchers have focused on stimulated radiation to control the stimulated radiation process through the optical cavity as well as to make it dominate in the light process to produce a variety of new laser sources [128]. In 1946, Purcell discovered that atoms that have spontaneous emission are not isolated but influenced by the environment [129]. From the classic theory, we can consider the excited state atoms on the outmost electrons as miniature antenna. Radiation occurs in the form of EM waves [130]. However, even if the atoms in the excited state are placed in the microcavity corresponding to its excitation wavelength, it is also possible that the radiated photons cannot be stored because the boundary condition cannot satisfy its resonance requirement. Therefore, spontaneous radiation is suppressed [131].

When the length of the cavity is equal to the half wavelength, the coherence between the spontaneous emission photons is obviously enhanced [132]. We consider an ideal microcavity, where all radiating photons are coupled into a single cavity resonant mode. When the coefficient of coupling of spontaneous radiation is infinitely close to 1, at this point, the laser output power and pump power are linearly related, and the threshold continues to decrease even to 0. For a closed cavity, the emission rate of a single atom can be expressed as

$$V_c = A(S+1)N \quad (23)$$

where A is the rate of spontaneous radiation and S and N are the number of photons and atoms, respectively. According to Equation (23), we can get the form of rate

$$\frac{dN}{dt} = H - A(S+1)N \quad (24)$$

and

$$\frac{dN}{dt} = A(S+1)N - \kappa s \quad (25)$$

where κs is the photon escape rate and H is the pump rate. The static solution of the equation

$$s = \frac{H}{\kappa} \text{ and } N = \frac{1}{A}\frac{H\kappa}{(H+\kappa)} \quad (26)$$

where $H = \kappa s$, the output light intensity is proportional to the pump rate; at this point, the laser operates in a thresholdless state. $H > \kappa$, the excited state atoms appear saturated at the κ/A level. Low threshold lasers are an important application of microcavity to control spontaneous emission [130, 133].

Achieving resonance requires an increase of probability of spontaneous emission at a particular wavelength by

adjusting the size of the microcavity, and the spontaneous emission becomes a reversible process.

4.4 Promotion of chemical reaction

The collective oscillations of the free electrons on the conductor surface form the SPs. The hybrid excitation is obtained by coupling the SPs to the phonons, which can be called SPP. SPP can propagate between the medium and the surface of metal until the energy gradually disappear [134]. Having described the basics of SPPs in Section 2, a number of applications controlling their propagation in the context of waveguiding are emerged, such as SPR sensors [135], SERS [136], cloaking [137], and photothermal cancer therapy [138]. Nowadays, plasmonics applied in chemical reactions has aroused widespread concerns.

Plasmons in the first 1–100 fs [73] follow landau damping. The thermal distribution of electron-hole pairs decays either through the reemission of photons or through carrier multiplication caused by electron-electron interactions [139]. Since 2010, Sun found the phenomenon that plasmon decay leads to the generation of hot electrons, which has been widely applied to research on plasmon-induced surface catalytic reactions [28]. However, the conversion efficiency between SPs and hot electrons is typically weaker [140]. Therefore, a challenge needs to be solved, which is finding a way to increase the conversion efficiency between SPs and hot electrons to accelerate chemical reaction.

Ding et al. [141] constructed a hybrid system of silver nanowire and graphene, which was used to promote chemical reactions by extending the electronic lifetime. The advantages of this hybrid device are shown in Figure 8 through ultrafast pump-probe transient absorption (UPPTRA) spectroscopy and surface reactions on this hybrid nanostructure.

In the visible region (VIS)-near-infrared region (NIR), UPPTRA spectroscopy was used. The femtosecond-resolved plasmon-exaction interaction of graphene-silver nanowire hybrids is experimentally investigated. From Table 1, the silver nanowire plasmonic lifetime is about 150 ± 7 fs. For monolayer graphene, the fast dynamic process at 275 ± 77 fs is due to the excitation of graphene excitons and the slow process at 1.4 ± 0.3 ps is due to the plasmonic hot electron interaction with photons of graphene. For the hybrid system of graphene-Ag nanowire, the time at which the hot electrons are transferred to the graphene via plasmon-induced is 534 ± 108 fs, and the time that graphene plasmon needs to be significantly enhanced through metal plasmon is about 3.2 ± 0.8 ps in the VIS, which can be used for plasmon-driven chemical reactions. This implies that the graphene-Ag nanowire hybrids can not only lead to a significant accumulation of high-density hot electrons but also significantly increase the plasmon-to-electron conversion efficiency due to the strong plasmon-exciton coupling.

5 Weak exciton-plasmon coupling

In 1974, Fleischmann first observed Raman signal enhancement [142] on the rough silver film surface, and this is also the first report on the interaction of SP and organic molecules. This finding facilitates the development of SERS. SP can achieve a great enhancement of the light field in a small scale to achieve the purpose of scattering enhancement [143]. Besides SERS, another important form of weak coupling is the SP-induced enhancement of molecular fluorescence, which is divided into SP-coupled emission enhancement (SPCE) [144] and SP-induced absorption enhancement [145], respectively. Nowadays, the study of SPCE characterizes steady-state spectroscopy.

In the weak coupling regime, EM modes and wave functions of plasmons and excitons are unperturbed during exciton-plasmon interaction, which is usually considered to be the SP EM field with the exciton dipole coupling [146]. Drexhage has used this model to study the change in the excitation decay rate of the emission dipole near the surface of the planar region [147]. In general, in the weak coupling regime, the well-known phenomenon includes increased radiation rate, enhanced adsorption cross-sections, and energy exchange between exciton and plasmon.

We refer to the three important parameters of rate associated with the coupling, which are traditionally called g (energy transfer rate between light and matter), γ' (rate of spontaneous emission into free-space in the cavity), different from γ, and κ (rate of light escape from the cavity), respectively. One of the two main systems of cavity-QED is weak coupling, which is different from strong coupling (g is the dominant). In the weak coupling regime, any of κ and γ' is greater than g.

Weak coupling has the characteristics of irreversible spontaneous emission, whether it is possibly suppressed [148] or enhanced [149], which makes it quite interesting.

5.1 Weak coupling conditions of cavity-QED

In 1995, Purcell [92] found that, when the atoms are in the microcavity or free space, there will be different

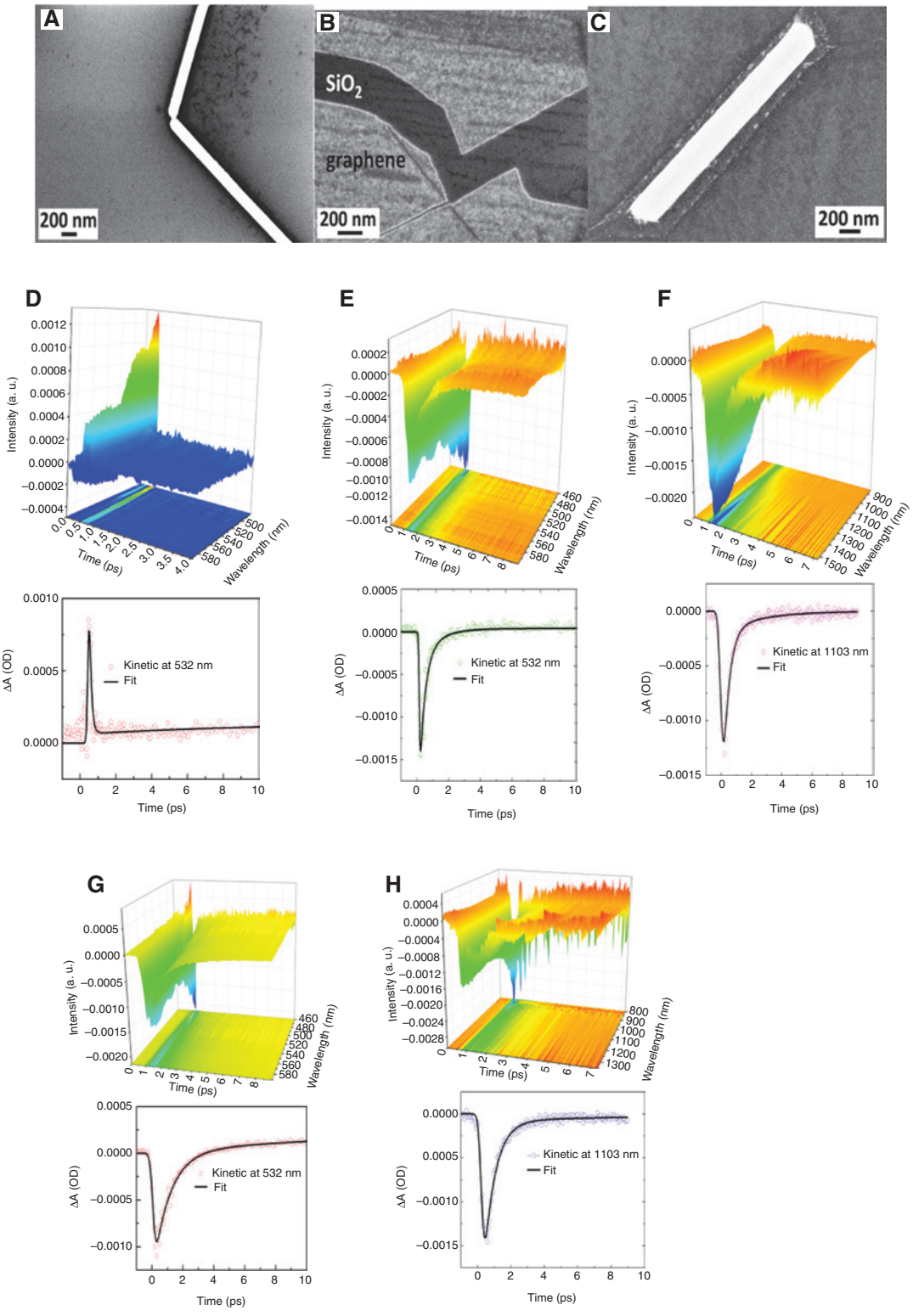

Figure 8: SEM image of silver nanowires, single-layer graphene, a single nanowire veiled with monolayer graphene, and UPPTRA spectroscopy.

(A–C) High-resolution SEM image of silver nanowires, graphene on SiO_2/Si substrate, and a single silver nanowire is hybridized with monolayer graphene, respectively. (D) UPPTRA spectroscopy of silver nanowires excited by laser, of which the high excitation wavelength is 400 nm and fitted dynamic curve at 532 nm. (E and F) UPPTRA spectroscopy of both VIS and NIR of graphene are excited by 400 nm laser and the dynamics was fitted at 532 and 1103 nm, respectively. (G and H) UPPTRA spectroscopy of both VIS and NIR of hybrid graphene are excited by 400 nm laser and the dynamics was fitted at 532 and 1103 nm, respectively.

Table 1: Fitted lifetimes of monolayer graphene, silver nanowires, and the hybrid system consist of silver nanowires and graphene detected in the VIS and NIR, respectively.

System	Spectrum range of probe light	Lifetime of fast process τ_1 (f_s)	Lifetime of slow process [τ_1 (p_s)]
Silver nanowires	VIS	150 ± 7 (4.4%)	
Graphene	VIS	275 ± 77 (22.4%)	1.4 ± 0.3 (27.9%)
Graphene	NIR	320 ± 46 (14.5%)	2.5 ± 0.6 (22.8%)
Silver nanowires/graphene	VIS	534 ± 108 (20.2%)	3.2 ± 0.8 (26.1%)
Silver nanowires/graphene	NIR	780 ± 92 (11.8%)	3.9 ± 0.9 (24.3%)

spontaneous emission rates and the rate of nuclear magnetic transition in the cavity will be increased. To sum up, we know that spontaneous emission depends on the emitter and environment, where *i* is located, rather than just one the factor. The ratio between the free space and modified (place the atoms in the cavity) emission rates is called the Purcell factor. The form of Purcell factor can be written as [150]

$$F_g = \frac{\gamma_g}{\gamma_0} \tag{27}$$

where γ_g and γ_0 are the spontaneous emission rate of the emitter that is not in the free space and that is in the free space, respectively.

As mentioned already, both the emitter and the environment will effect decay rate γ and are spilt into two terms (decay rate from the excited state to the final state). We can use Fermi's golden rule to calculate the radiation rate transition [151]:

$$\gamma = 2\pi \frac{\rho(\omega)}{\hbar^2} |\langle i | \hat{E}_{\text{cav}} \cdot \hat{\mu} | j \rangle|^2 \tag{28}$$

$|j\rangle$ and $|i\rangle$ are the initial (excited) and the final state, respectively. $\hat{\mu}$ is the electric dipole, $\hat{E}_{\text{cav}}$ is the operator of vacuum field, and $\rho(\omega)$ is the final state density of photonic. One can calculated $\rho(\omega)$ in vacuum by considering the EM modes within a cube of volume *V*,

$$\rho(\omega) = \rho_0 V = \frac{\omega^2 V}{c^3 \pi^2} \tag{29}$$

Note that *V* is arbitrary volume, which serves as a tool and will disappear. ρ_0 is the local density of states for vacuum. On the contrary, the transition matrix element in Equation (23), averaged over all the possible direction, yields

$$|\langle i | \hat{E}_{\text{cav}} \cdot \hat{\mu} | j \rangle|^2 = \frac{(E_{\text{cav}} \cdot \mu_{ij})^2}{3} \tag{30}$$

$$\mu_{ij} = -e\langle i | r | j \rangle \tag{31}$$

where *r* is the position operator and *e* is the electron charge. E_{cav} is the vacuum electric field, which can be obtained from

$$\int \varepsilon_0 {E_{\text{cav}}}^2 dV = \frac{1}{2}\hbar\omega \tag{32}$$

So,

$$E_{\text{cav}} = \frac{\sqrt{2}}{2} \cdot \left(\frac{\hbar\omega}{V\varepsilon_0} \right)^{-\frac{1}{2}} \tag{33}$$

By combing the above equation, we can get the spontaneous emission rate of the emitter in the free space:

$$\gamma_0 = \frac{1}{3} \frac{{\mu_{ij}}^2 \omega^3}{\hbar \pi \varepsilon_0 c^3} \tag{34}$$

In Equation (23), we can see that the zero-point fluctuation of the EM field can cause the spontaneous emission of the excited state.

The same results happen when we place the emitter in the cavity [152, 153]. As the cavity itself can have different scales, shapes, and components, only specific modes of EM will be supported [154]. In short, if we only provided a cavity with only one single frequency, ω_c, the states density, can be presented by the Lorentz equation:

$$\rho(\omega) = \frac{1}{2\pi} \cdot \frac{\Delta\omega}{\Delta\omega^2 + (\omega - \omega_c)^2} \tag{35}$$

where $\Delta\omega$ is the width of the local density of states maximum at $\omega = \omega_c$. If we place an emitter into the cavity, $\omega_0 = \omega_c$, the occurrence of electronic transition, the cavity is tuned to the emission frequency, and the density of states $\rho(\omega_0)$ can be written as

$$\rho(\omega_0) = \frac{2}{\pi} \cdot \frac{\omega_c}{\omega_0 \Delta\omega} = \frac{2Q}{\omega_0 \pi} \tag{36}$$

Using Equations (24) and (30), we can also obtain the rate of decay of an emitter placed within a microcavity.

$$\gamma_g = \frac{2}{3}\frac{\mu_{ij}^2 Q}{\varepsilon_0 \hbar V} \tag{37}$$

Through Equations (21), (28), and (31), we can get the new concrete expression of the factor

$$F_g = \frac{3}{4}\frac{Q\lambda^3}{\pi V} \tag{38}$$

V is the volume of the cavity, Q is the quality factor of the cavity, and λ is the wavelength related to the transition. F_g describes how the presence of a cavity changes the spontaneous emission rate of the emitter. If $F_g < 1$, the spontaneous emission rate is inhibited; otherwise, the cavity enhances the emission. This formula of Equation (29) shows that the optical resonator can significantly increase the emission rate while compressing the light to a small range and storing it for a long time [155, 156]. However, the realization of these two goals in the strict sense is contradictory, because the tighter confinement is always accompanied by high losses. At present, the modification of the emission characteristics is mainly focused on the study of resonators.

5.2 Application of weak coupling

The spontaneous emission of the material is due to the fact that the material itself interacts with the local EM rather than the inherent properties of materials [157]. The characteristics of spontaneous emission can be modified by changing the field of local EM [158]. Plasma metal nanoparticles and photonic crystals are two core structures of nanophotonics; the main effort is to change the spontaneous emission [159]. Although the technique of modifying spontaneous emission was achieved in 40 years, its importance in the transition from photonics to nanophotonics is increasing nowadays. Besides, the length of optical structure is shorter than light.

5.2.1 SERS

SERS spectroscopy is developed in the field of metal plasma. The SERS effect is due to the fact that the molecules are absorbed on the rough metal surface and the scattering is greatly enhanced [160–163]. The effects of SERS are generally divided into types, which are chemical enhancements and physical enhancements, respectively. The mechanism involves the excitation of the SP and chemical enhancement is associated with charge transfer, also known as charge transfer resonance Raman [29, 164, 165]. When the incident light illuminates the metal surface, metal nanostructures have the ability to compress light into a small volume between two nanoparticles, and the EM field strength of the region is greatly enhanced to produce a hotspot (see Figure 9) [167, 168].

Under the mechanism of EM enhancement, the factor of SERS enhancement factor can be expressed as [169]

$$G_{\mathrm{EM}} = \sigma(\omega_1)\sigma(\omega_2) \tag{39}$$

where $\sigma = |E_L|^2 / |E_I|^2$, and ω_1 and ω_2 are the frequencies of pump and Raman shifted, respectively. From Equation (39), the magnitude of the enhancement factor depends on the local EM field enhancement.

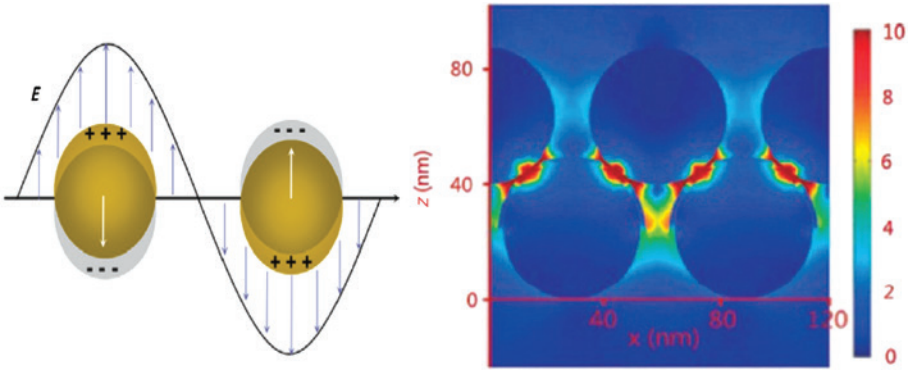

Figure 9: Sketch of the mechanism of laser irradiation to gold or sliver nanostructured surfaces.
The left image shows local surface plasmas caused by collective oscillations of charge on the surface of metal nanoparticles [47]. The right image is the distribution of the EM field intensity, which is simulated by the finite element method [166].

When ω_2 is much smaller than ω_1, from Equation (39),

$$G_{EM} = |E_L|^4 / |E_I|^4 \tag{40}$$

From Equation (40), the enhancement factor can reach ~10^6, even up to ~10^{10}–10^{12}. If the isolated molecular Raman scattering is very low, it can be used to achieve the purpose of single molecule detection [170–172]. Although SERS has demonstrated great potential in the field of molecular detection, the difference in the surface roughness of the metal and the difference in the absorption position of molecules on the metal surface result in a nonreproducibility of the experiments. Therefore, the precisely controllable metal nanometer arrays are used as substrates [173].

Here, we introduce a kind of technology shell-isolated nanoparticle-enhanced Raman spectroscopy (SHINERS). Michaels et al. [174] have constructed a core-shell structure with ultrathin alumina or silica-coated gold nanoparticles (see Figure 10).

The advantages of the structure are as follows: (1) The coverage of the ultrathin layer can prevent the aggregation of metal nanoparticles. (2) The material can be detected in direct contact with the substrate. (3) The nanoparticles conform to different substrate profiles [175]. The yeast cells were measured through this technique and high-quality molecular Raman spectroscopy can be obtained (see Figure 11).

The measurement of yeast cells and research show that the technology is greatly promoted in the life sciences and materials in the field of SERS applications, and even related to food safety testing, explosives, environmental pollution, and so on.

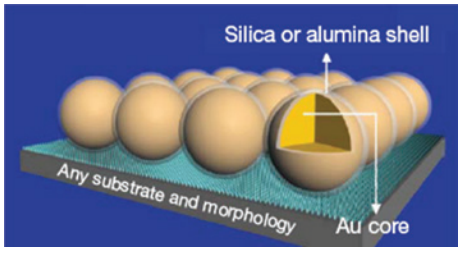

Figure 10: Simple schematic diagram covers gold nanoparticles with ultrathin alumina and silica layers.

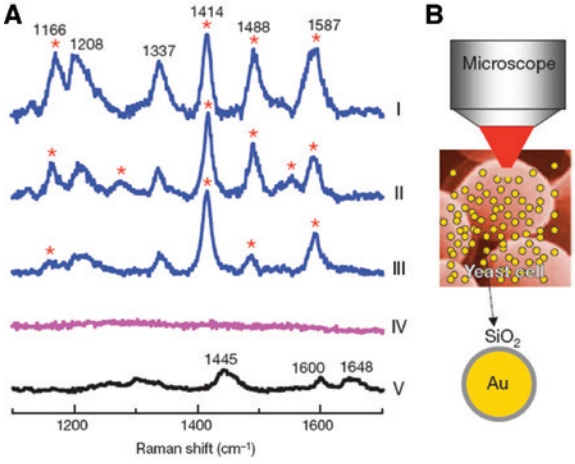

Figure 11: Schematic diagram shows that the biological structure of yeast cells is detected in situ by SHINERS.
(A) Under this mechanism, the molecular Raman spectra (curves I–III) are obtained with different hotspots. In curve IV, there is no molecular adsorption substrate. Curve V shows the Raman spectra of yeast cells themselves. (B) Schematic of a SHINERS experiment on living yeast cells [176].

5.2.2 Surface-enhanced fluorescence

Over the past decade, the interaction of metals and fluorescent substances has become one of the hottest research areas [177–179]. When the incident light is irradiated onto the surface of the metal nanostructure, it will react with the subwavelength metal and the fluorescent groups are adsorbed on the metal surface. The metal-generated SPs can greatly increase the luminous intensity of the fluorescent substance [180]. The enhancement of the local electric field is due to the fact that the optical cross-section of the gold and silver subwavelength particles is many times larger than the geometric scattering cross-section [181]. The interaction of the plasmons with the fluorescent substance can improve the luminescence rate of the material [182], reduce the fluorescence lifetime [183], and improve the light stability of the luminescent material [184].

We assume that the fluorescent molecule is attached to the metal surface and that its fluorescence detection signal enhancement can be expressed as [185]

$$F = \frac{\eta \left|\mu \cdot E_L\right|^2}{\eta_0 \left|\mu \cdot E\right|^2} \tag{41}$$

It can be seen from the above equation that the incident light intensity E and the local electric field intensity play a decisive role in the enhancement mechanism. η is the quantum efficiency, which can be written as

$$\eta = \frac{\gamma_R}{\gamma_T} \tag{42}$$

where γ_R is the rate of radiative rate and γ_T is the rate of total decay of the molecule. $\gamma_T = \gamma_R + \gamma_{NR}$, where γ_{NR} is the nonradiative decay rate.

From Equation (41), we can conclude that the fluorescence will be greatly enhanced when both the quantum efficiency and the local EM field are amplified (see Figure 12).

Yang et al. constructed a hybrid system of molybdenum disulfide (MoS_2) and silver nanoparticles (AgNPs), and by adjusting the diameter of the metal particles, different fluorescence enhancement results have been obtained (see Figure 13).

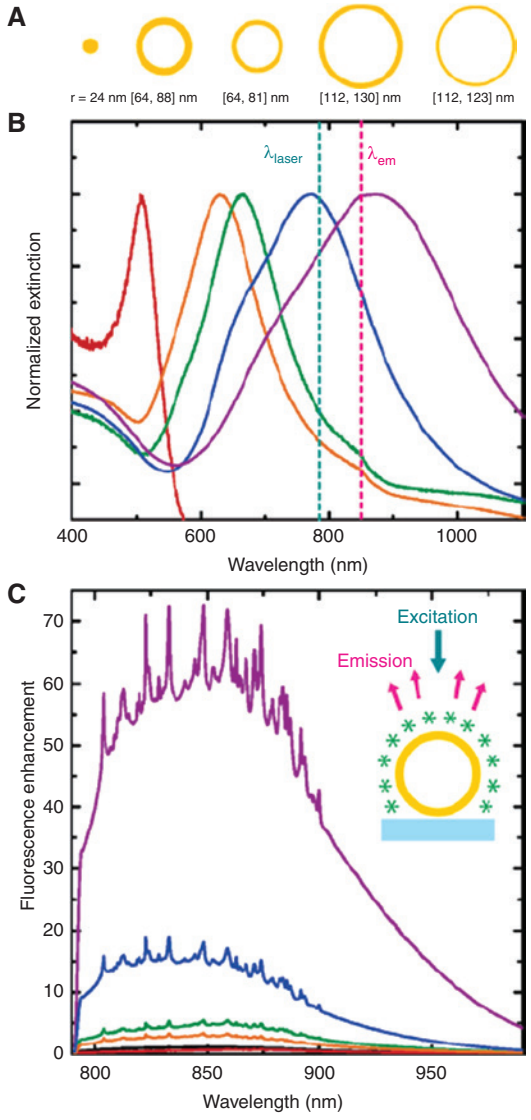

Figure 12: Schematics of the relation between Raman intensity and diameter of gold nanoparticles.
(A) Schematic of gold nanoparticles (colloidal and core-shell) as a substrate to enhance fluorescence. (B) Spectral measurements corresponding to the different metal nanoparticles in (A) as substrate. (C) Fluorescence spectra of indocyanine green (ICG) combined with substrates of different nanostructures, adjusted for surface area to be available for fluorophore conjugation. The black curve represents the fluorescence of ICG without metal nanoparticles [176].

The metal nanostructures can influence the fluorescence emission of molecules [187], and the radiation decay rate of the molecules [188] and the scattering of nanostructures are changed by increasing the coupling efficiency of fluorescence emission to far field [189]. All processes can be controlled by the distance, size, and geometric parameters between the particles.

The shortcomings of limited brightness and spatial diffraction limits can be conquered by locally exciting surface plasmas [190]. Importantly, the quantum efficiency and local electric field enhancement lead to the increase of fluorescence. Metal surface-enhanced fluorescence in many ways reflects its extraordinary characteristic. However, it is worth mentioning the urgent problem that the experimental value is not consistent with the theoretical results. It is impossible to achieve optimal enhancement in the experiment. For example, to enhance the excitation process, in the optical frequency space, there must be an overlap among the metal SPR peak, molecular absorption band, and excitation wavelength. However, SPR frequency is affected by the surrounding medium. From the basic disciplines through the construction of metal nanostructures, to achieve the regulation of spontaneous radiation is of great significance. It shows a lot of application potentials in many areas and is gradually infiltrated into the practical field.

5.2.3 Solar cells

Photovoltaic (PV) cells can convert light into electrical energy. In contemporary social development, the emergency of PV helps solve the problem of energy shortages [191]. However, to make PV technology dominate, the primary goal is to reduce costs. At present, most of the solar cells are produced by the crystal silicon, so the main cost is silicon processing and production [192–194]. In view of the cost, there is great interest in thin-film cells that are deposited on cheap substrates. But for now, only by the use of less silicon to reduce costs is accompanied by the emergence of the problem that the conversion efficiency will be affected.

It is generally believed that light is absorbed by all and the light carriers are collected, so the photoelectric absorber must be thick at the optical level [195]. In the field of PV, usually with the semiconductor as the absorber, its optical thickness is generally several times shorter than the length of light absorption, such as silicon [196, 197]. Moreover, the diffusion length of the carrier is greater than the thickness of the material that must be available for high-efficiency cells (see Figure 14).

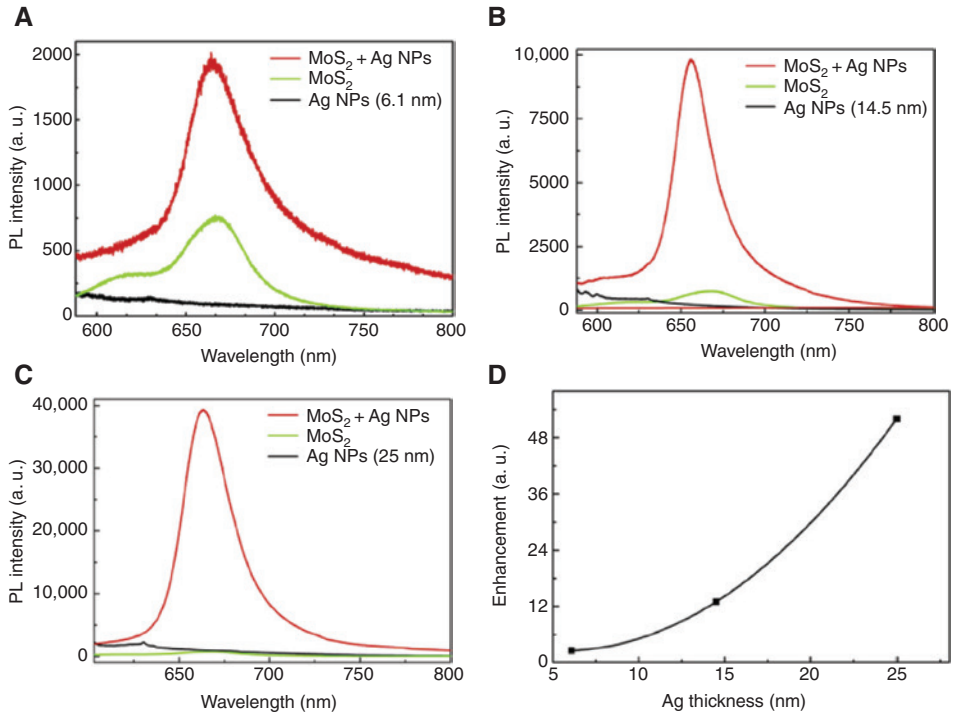

Figure 13: Schematics of the relation between the fluorescence intensity and the diameter of gold nanoparticles.
(A–C) LSPR on the surface of different diameter metal particles, and different fluorescence enhancement results can be obtained, where the diameters of AgNPs are 6, 14, and 25 nm, respectively. (D) Enhancement factors for different thicknesses [186].

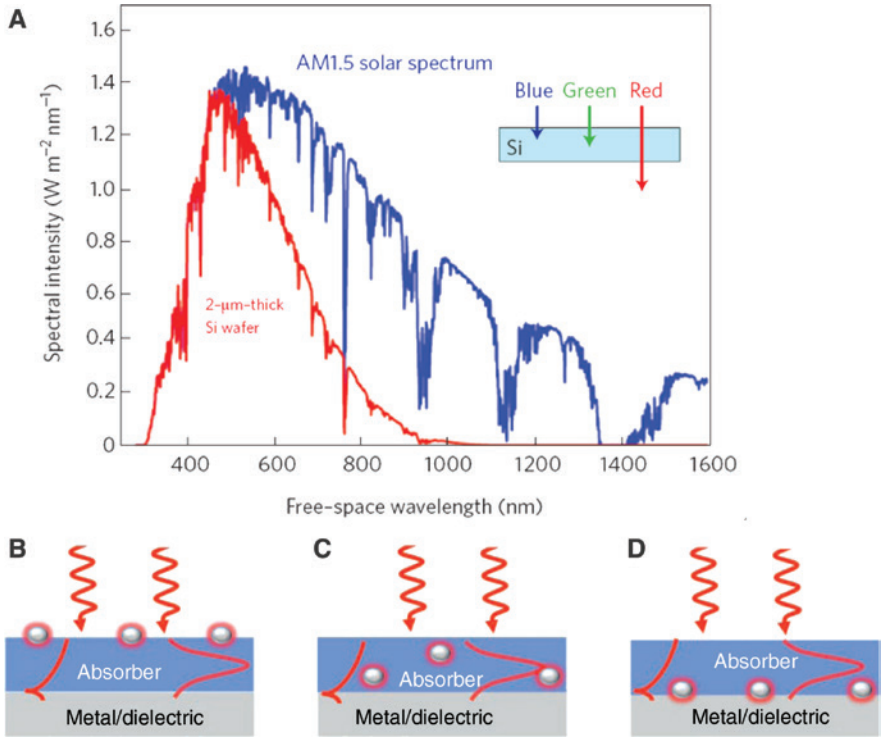

Figure 14: Schematics of the absorption AM1.5 solar spectrum and the mechanism of configurations.
(A) Schematic diagram of the absorption of AM1.5 solar spectra at different thicknesses in a 2-μm-thick crystalline silicon film [195]. Generalized scatterers for coupling into waveguide modes in a solar cell. Scatterers can consist of particles on top (B), middle (C), or back (D) of the solar cell and could contain layers of metal, dielectrics, transparent conducting oxides, or air on the back surface. Incident sunlight is then scattered into photonic or SPP modes depending on the scattering object and incident wavelength of light [198].

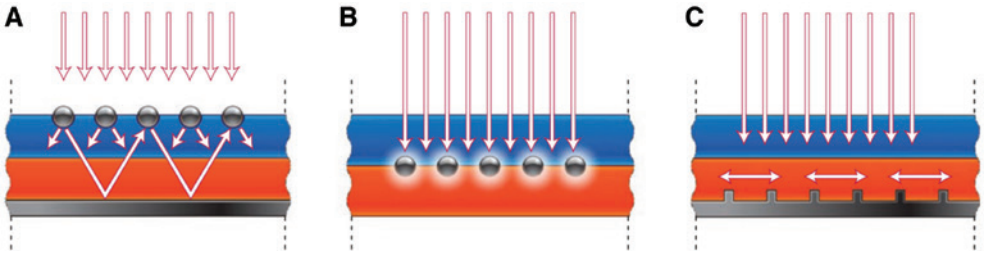

Figure 15: Schematic diagram of plasma capture light for a thin-film solar cells.
(A) Using the metal nanostructure scattering characteristics to achieve the purpose of light capture. (B) Metal nanoparticles embedded in the semiconductor for producing local surface plasmas to capture light. (C) Incident light is irradiated onto the metal surface to produce an SP polarization effect that promotes light absorption [195].

As shown in Figure 14, clearly most of the incident light in the range of 600–1100 nm cannot be absorbed by the solar cells with silicon crystal film. The new technology that uses nanoscale metal substrates can achieve thin-film solar cells for light capture (see Figure 15).

Here, we show three types of configurations (see Figure 14). The light is captured and stored in the semiconductor using the scattering characteristics of the light on the metal nanoparticles. According to the local electric field, it is proportional to the absorption of the semiconductor [199]. The metal nanoparticles are deposited or even embedded in the semiconductor, and metal nanoparticles on the regulation of light characteristics are used to increase the absorption of incident light by increasing the local electric field [200–202]. The incident light is coupled with the nanoparticles in the form of waveguides between the nanoparticles and the medium until the light is completely absorbed [203–205].

Plasmonics interconnects would be a great for solar cells. The propagation and localization of light at the nanometer scale are realized in the field of plasmonics [206, 207]. In view of the special nature of plasmonics, researchers began to turn their attention to the plasmon application to the field of solar cells. The introduction of a plasmonic cell design concept in a solar cell study can greatly increase the absorptivity of light to PV devices, and the thickness of the PV device absorption layer requirements is greatly reduced. This discovery paves the way toward the development solar cells.

6 Conclusions

In this review, we first showed the definition of the plasmon and its unique aspects of light operation. Then, we presented the exciton coupling with the plasmon and included the coupling classification as well as the application in various fields, such as biological, chemical, and quantum information fields. The concept of coupling has been of interest to a vast number of researchers since the presentation. A lot of research and development have been made in this field.

Acknowledgments: This work was supported by the National Natural Science Foundation of China (grant nos. 11374353 and 91436102), Municipal Science and Technology Project (grant no. Z17111000220000), National Basic Research Program of China (grant no. 2016YFA02008000), and Taishan Scholar Project of Shandong Province, Project of Shandong Province Higher Educational Science and Technology Program (grant no. J17KA186).

References

[1] Frenkel J. On the transformation of light into heat in solids. I. Phys Rev 1931;37:17–44.
[2] Yablonovitch E. Inhibited spontaneous emission in solid-state physics and electronics. Phys Rev Lett 1987;58:2059–62.
[3] Liu GB, Xiao D, Yao Y, Xu X, Yao, W. Electronic structures and theoretical modelling of two-dimensional group-VIB transition metal dichalcogenides. Chem Soc Rev 2015;44:2643–63.
[4] Ritchie RH. Plasma losses by fast electrons in thin films. Phys Rev 1957;106:874–81.
[5] Zhang Z, Fang Y, Wang W, Chen L, Sun M. Propagating surface plasmon polaritons: towards applications for remote-excitation surface catalytic reactions. Adv Sci (Weinh) 2016;3:1500215.
[6] Zhao W, Wang S, Liu B, et al. Exciton-plasmon coupling and electromagnetically induced transparency in monolayer semiconductors hybridized with Ag nanoparticles. Adv Mater 2016;28:2709–15.
[7] Moskovits M. Surface-enhanced spectroscopy. Rev Mod Phys 1985;57:783–826.
[8] Brockman JM, Nelson BP, Corn RM. Surface plasmon resonance imaging measurements of ultrathin organic films. Annu Rev Phys Chem 2000;51:41–63.
[9] Bellessa J, Bonnand C, Plenet JC, Mugnier J. Strong coupling between surface plasmons and excitons in an organic semiconductor. Phys Rev Lett 2004;93:036404.

[10] Dintinger J, Klein S, Bustos F, Barnes WL, Ebbesen TW. Strong coupling between surface plasmon-polaritons and organic molecules in subwavelength hole arrays. Phys Rev B 2005;71:035424.
[11] Schlather AE, Large N, Urban AS, Nordlander P, Halas NJ. Near-field mediated plexcitonic coupling and giant Rabi splitting in individual metallic dimers. Nano Lett 2013;13:3281–6.
[12] Cheng CW, Sie EJ, Liu B, et al. Surface plasmon enhanced band edge luminescence of ZnO nanorods by capping Au nanoparticles. Appl Phys Lett 2010;96:071107.
[13] Manjavacas A, Garcia de Abajo FJ, Nordlander P. Quantum plexcitonics: strongly interacting plasmons and excitons. Nano Lett 2011;11:2318–23.
[14] Fofang NT, Grady NK, Fan Z, Govorov AO, Halas NJ, et al. Plexciton dynamics: exciton-plasmon coupling in a J-aggregate-Au nanoshell complex provides a mechanism for nonlinearity. Nano Lett 2011;11:1556–60.
[15] Fedutik Y, Temnov VV, Schöps O, Woggon U, Artemyev MV. Exciton-plasmon-photon conversion in plasmonic nanostructures. Phys Rev Lett 2007;99:136802.
[16] Akimov AV, Mukherjee A, Yu CL, et al. Generation of single optical plasmons in metallic nanowires coupled to quantum dots. Nature 2007;450:402–6.
[17] Chang D, Sørensen AS, Hemmer PR, Lukin MD. Quantum optics with surface plasmons. Phys Rev Lett 2006;97:053002.
[18] Ditlbacher H, Hohenau A, Wagner D, et al. Silver nanowires as surface plasmon resonators. Phys Rev Lett 2005;95:257403.
[19] Gramotnev DK, Bozhevolnyi SI. Plasmonics beyond the diffraction limit. Nat Photon 2010;4:83–91.
[20] Tame MS, McEnery KR, Özdemir ŞK, et al. Quantum plasmonics. Nat Phys 2013;9:329–40.
[21] Wang L-L, Zou CL, Ren XF, et al. Exciton-plasmon-photon conversion in silver nanowire: polarization dependence. Appl Phys Lett 2011;99:061103.
[22] Kolesov R, Grotz B, Balasubramanian G, et al. Wave-particle duality of single surface plasmon polaritons. Nat Phys 2009;5:470–4.
[23] Dai D, Dong Z, Fan J. Giant photoluminescence enhancement in SiC nanocrystals by resonant semiconductor exciton-metal surface plasmon coupling. Nanotechnology 2013;24:025201.
[24] Govorov AO, Lee J, Kotov NA. Theory of plasmon-enhanced Förster energy transfer in optically excited semiconductor and metal nanoparticles. Phys Rev B 2007;76:125308.
[25] Vasa P, Pomraenke R, Schwieger S, et al. Coherent exciton-surface-plasmon-polariton interaction in hybrid metal-semiconductor nanostructures. Phys Rev Lett 2008;101:116801.
[26] Sun M, Xu H. A novel application of plasmonics: plasmon-driven surface-catalyzed reactions. Small 2012;8:2777–86.
[27] Sun M, Zhang Z, Zheng H, Xu H. In-situ plasmon-driven chemical reactions revealed by high vacuum tip-enhanced Raman spectroscopy. Sci Rep 2012;2:647.
[28] Fang Y, Li Y, Xu H, Sun M. Ascertaining *p*,*p*′-dimercaptoazobenzene produced from *p*-aminothiophenol by selective catalytic coupling reaction on silver nanoparticles. Langmuir 2010;26:7737–46.
[29] Sun M, Liu S, Chen M, Xu H. Direct visual evidence for the chemical mechanism of surface-enhanced resonance Raman scattering via charge transfer. J Raman Spectrosc 2009;40:137–43.
[30] Sun M, Wan S, Liu Y, Jia Y, Xu H. Chemical mechanism of surface-enhanced resonance Raman scattering via charge transfer in pyridine-Ag_2 complex. J Raman Spectrosc 2008;39:402–8.
[31] Wurtz GA, Evans PR, Hendren W, et al. Molecular plasmonics with tunable exciton-plasmon coupling strength in J-aggregate hybridized Au nanorod assemblies. Nano Lett 2007;7:1297–303.
[32] Savasta S, Saija R, Ridolfo A, Di Stefano O, Denti P, Borghese F. Nanopolaritons: vacuum Rabi splitting with a single quantum dot in the center of a dimer nanoantenna. ACS Nano 2010;4:6369–76.
[33] Artuso RD, Bryant GW. Optical response of strongly coupled quantum dot-metal nanoparticle systems: double peaked Fano structure and bistability. Nano Lett 2008;8:2106–11.
[34] Zengin G, Johansson G, Johansson P, Antosiewicz TJ, Käll M, Shegai T. Approaching the strong coupling limit in single plasmonic nanorods interacting with J-aggregates. Sci Rep 2013;3:3074.
[35] Haes AJ, Zou S, Zhao J, Schatz GC, Van Duyne RP. Localized surface plasmon resonance spectroscopy near molecular resonances. J Am Chem Soc 2006;128:10905–14.
[36] Zhao J, Jensen L, Sung J, Zou S, Schatz GC, Van Duyne RP. Interaction of plasmon and molecular resonances for rhodamine 6G adsorbed on silver nanoparticles. J Am Chem Soc 2007;129:7647–56.
[37] Zheng YB, Kiraly B, Cheunkar S, Huang TJ, Weiss PS. Incident-angle-modulated molecular plasmonic switches: a case of weak exciton-plasmon coupling. Nano Lett 2011;11:2061–5.
[38] Halas NJ, Lal S, Chang WS, Link S, Nordlander P. Plasmons in strongly coupled metallic nanostructures. Chem Rev 2011;111:3913–61.
[39] Giannini V, Fernández-Domínguez AI, Sonnefraud Y, Roschuk T, Fernández-García R, Maier SA. Controlling light localization and light-matter interactions with nanoplasmonics. Small 2010;6:2498–507.
[40] Johnson PB, Christy RW. Optical constants of the noble metals. Phys Rev B 1972;6:4370–9.
[41] Fofang NT, Park TH, Neumann O, Mirin NA, Nordlander P, Halas NJ. Plexcitonic nanoparticles: plasmon-exciton coupling in nanoshell-J-aggregate complexes. Nano Lett 2008;8:3481–7.
[42] Rakovich A, Albella P, Maier SA. Plasmonic control of radiative properties of semiconductor quantum dots coupled to plasmonic ring cavities. ACS Nano 2015;9:2648–58.
[43] García MA. Surface plasmons in metallic nanoparticles: fundamentals and applications. J Phys D Appl Phys 2011;44:283001.
[44] Schuurmans FJP, de Lang, DTN, Wegdam GH, Sprik R, Lagendijk A. Local-field effects on spontaneous emission in a dense supercritical gas. Phys Rev Lett 1998;80:5077.
[45] Ding Q, Chen M, Li Y, Sun M. Effect of aqueous and ambient atmospheric environments on plasmon-driven selective reduction reactions. Sci Rep 2015;5:10269.
[46] Cui L, Wang P, Li Y, Sun M. Selective plasmon-driven catalysis for para-nitroaniline in aqueous environments. Sci Rep 2016;6:20458.
[47] Zhang Z, Silkin VM, Chulkov EV, Echenique PM. Surface plasmon-driven photocatalysis in ambient, aqueous and high-vacuum monitored by SERS and TERS. J Photochem Photobiol C Photochem Rev 2016;27:100–12.
[48] Pitarke J, Xu P, Yang X, Liang W, Sun M. Theory of surface plasmons and surface-plasmon polaritons. Rep Prog Phys 2006;70:1.

[49] Lagois J, Fischer B. Experimental observation of surface exciton polaritons. Phys Rev Lett 1976;36:680–3.
[50] Yang F, Sambles JR, Bradberry GW. Long-range coupled surface exciton polaritons. Phys Rev Lett 1990;64:559–62.
[51] Cramer T, Wanner A, Gumbsch P. Crack velocities during dynamic fracture of glass and single crystalline silicon. Phys Stat Solidi A 1997;164:R5–6.
[52] Agranovich V, Benisty H, Weisbuch C. Organic and inorganic quantum wells in a microcavity: Frenkel-Wannier-Mott excitons hybridization and energy transformation. Solid State Commun 1997;102:631–6.
[53] Rohlfing M, Louie SG. Excitons and optical spectrum of the Si (111)-(2×1) surface. Phys Rev Lett 1999;83:856.
[54] Turlet JM, Philpott MR. Surface and bulk exciton transitions in the reflection spectrum of tetracene crystals. J Chem Phys 1975;62:4260–5.
[55] DeMartini F, Colocci M, Kohn SE, Shen YR. Nonlinear optical excitation of surface exciton polaritons in ZnO. Phys Rev Lett 1977;38:1223–6.
[56] Sheik-Bahae M, Said AA, Wei TH, Hagan DJ, Van Stryland EW. Sensitive measurement of optical nonlinearities using a single beam. IEEE J Quantum Electron 1990;26:760–9.
[57] Morel A, Bricaud A. Theoretical results concerning light absorption in a discrete medium, and application to specific absorption of phytoplankton. Deep Sea Res Pt A Oceanogr Res Pap 1981;28:1375–93.
[58] Sugawara Y, Kelf TA, Baumberg JJ, Abdelsalam ME, Bartlett PN. Strong coupling between localized plasmons and organic excitons in metal nanovoids. Phys Rev Lett 2006;97:266808.
[59] Hakala T, Toppari JJ, Kuzyk A, et al. Vacuum Rabi splitting and strong-coupling dynamics for surface-plasmon polaritons and rhodamine 6G molecules. Phys Rev Lett 2009;103:053602.
[60] Reithmaier JP, Sęk G, Löffler A, et al. Strong coupling in a single quantum dot-semiconductor microcavity system. Nature 2004;432:197–200.
[61] Pockrand I, Swalen JD, Gordon JG, Philpott MR. Exciton-surface plasmon interactions. J Chem Phys 1979;70:3401–8.
[62] Cui L, Wang P, Fang Y, Li Y, Sun M. A plasmon-driven selective surface catalytic reaction revealed by surface-enhanced Raman scattering in an electrochemical environment. Sci Rep 2015;5:11920.
[63] Pompa PP, Martiradonna L, Della Torre A, et al. Metal-enhanced fluorescence of colloidal nanocrystals with nanoscale control. Nat Nanotechnol 2006;1:126–30.
[64] Dulkeith E, Morteani AC, Niedereichholz T, et al. Fluorescence quenching of dye molecules near gold nanoparticles: radiative and nonradiative effects. Phys Rev Lett 2002;89:203002.
[65] Lambright S, Butaeva E, Razgoniaeva N, et al. Enhanced lifetime of excitons in nonepitaxial Au/CdS core/shell nanocrystals. ACS Nano 2013;8:352–61.
[66] Ming T, Chen H, Jiang R, Li Q, Wang J. Plasmon-controlled fluorescence: beyond the intensity enhancement. J Phys Chem Lett 2012;3:191–202.
[67] Wang H, Liu T, Huang Y, et al. Plasmon-driven surface catalysis in hybridized plasmonic gap modes. Sci Rep 2014;4:7087.
[68] Zhang W, Govorov AO, Bryant GW. Semiconductor-metal nanoparticle molecules: hybrid excitons and the nonlinear Fano effect. Phys Rev Lett 2006;97:146804.
[69] Boca A, Miller R, Birnbaum KM, Boozer AD, McKeever J, Kimble HJ. Observation of the vacuum Rabi spectrum for one trapped atom. Phys Rev Lett 2004;93:233603.
[70] Antoine-Vincent N, Natali F, Byrne D, et al. Observation of Rabi splitting in a bulk GaN microcavity grown on silicon. Phys Rev B 2003;68:153313.
[71] Médard F, Zúñiga-Pérez J, Disseix P, et al. Experimental observation of strong light-matter coupling in ZnO microcavities: influence of large excitonic absorption. Phys Rev B 2009;79:125302.
[72] Lai CW, Kim NY, Utsunomiya S, et al. Coherent zero-state and pi-state in an exciton-polariton condensate array. Nature 2007;450:529–32.
[73] Liu X, Galfsky T, Sun Z, et al. Strong light-matter coupling in two-dimensional atomic crystals. Nat Photon 2015;9:30–4.
[74] Liu W, Lee B, Naylor CH, et al. Strong exciton-plasmon coupling in MoS_2 coupled with plasmonic lattice. Nano Lett 2016;16:1262–9.
[75] Porras D, Ciuti C, Baumberg JJ, Tejedor C. Polariton dynamics and Bose-Einstein condensation in semiconductor microcavities. Phys Rev B 2002;66:085304.
[76] Hennessy K, Badolato A, Winger M, et al. Quantum nature of a strongly coupled single quantum dot-cavity system. Nature 2007;445:896–9.
[77] Wei H, Ratchford D, Li X, Xu H, Shih CK. Propagating surface plasmon induced photon emission from quantum dots. Nano Lett 2009;9:4168–71.
[78] Xia K, Twamley J. All-optical switching and router via the direct quantum control of coupling between cavity modes. Phys Rev X 2013;3:031013.
[79] McKeever J, Boca A, Boozer AD, Buck JR, Kimble HJ. Experimental realization of a one-atom laser in the regime of strong coupling. Nature 2003;425:268–71.
[80] Chang DE, Sørensen AS, Demler EA, Lukin MD. A single-photon transistor using nanoscale surface plasmons. Nat Phys 2007;3:807–12.
[81] Dufferwiel S, Schwarz S, Withers F, et al. Exciton-polaritons in van der Waals heterostructures embedded in tunable microcavities. Nat Commun 2015;6:8579.
[82] Tischler JR, Bradley MS, Zhang Q, Atay T, Nurmikko A, Bulović V. Solid state cavity QED: strong coupling in organic thin films. Org Electron 2007;8:94–113.
[83] Schülzgen A, Binder R, Donovan ME, et al. Direct observation of excitonic Rabi oscillations in semiconductors. Phys Rev Lett 1999;82:2346.
[84] John S. Strong localization of photons in certain disordered dielectric superlattices. Phys Rev Lett 1987;58:2486–9.
[85] Yokoyama H, Nishi K, Anan T, et al. Enhanced spontaneous emission from GaAs quantum wells in monolithic microcavities. Appl Phys Lett 1990;57:2814–6.
[86] Yamauchi T, Arakawa Y, Nishioka M. Enhanced and inhibited spontaneous emission in GaAs/AlGaAs vertical microcavity lasers with two kinds of quantum wells. Appl Phys Lett 1991;58:2339–41.
[87] Raizen M, Thompson RJ, Brecha RJ, Kimble HJ, Carmichael HJ. Normal-mode splitting and linewidth averaging for two-state atoms in an optical cavity. Phys Rev Lett 1989;63:240.
[88] Sanchez-Mondragon JJ, Narozhny NB, Eberly JH. Theory of spontaneous-emission line shape in an ideal cavity. Phys Rev Lett 1983;51:550–3.
[89] Agarwal GS. Vacuum-field Rabi oscillations of atoms in a cavity. J Opt Soc Am B 1985;2:480–5.

[90] Zhu Y, Gauthier DJ, Morin SE, Wu Q, Carmichael HJ, Mossberg TW. Vacuum Rabi splitting as a feature of linear-dispersion theory: analysis and experimental observations. Phys Rev Lett 1990;64:2499–502.
[91] Weisbuch C, Nishioka M, Ishikawa A, Arakawa Y. Observation of the coupled exciton-photon mode splitting in a semiconductor quantum microcavity. Phys Rev Lett 1992;69:3314–7.
[92] Purcell EM. Spontaneous emission probabilities at radio frequencies. In: Burstein E., Weisbuch C. eds. Confined electrons and photons. NATO ASI Series (Series B: Physics), 1995, 340. Boston, MA: Springer.
[93] Milonni PW, Knight P. Spontaneous emission between mirrors. Opt Commun 1973;9:119–22.
[94] Hulet RG, Hilfer ES, Kleppner D. Inhibited spontaneous emission by a Rydberg atom. Phys Rev Lett 1985;55:2137–40.
[95] Kimble HJ. Strong interactions of single atoms and photons in cavity QED Phys Scr 1998;1998:127.
[96] Hood C, Lynn TW, Doherty AC, Parkins AS, Kimble HJ. The atom-cavity microscope: single atoms bound in orbit by single photons. Science 2000;287:1447–53.
[97] Zheng S-B, Guo G-C. Efficient scheme for two-atom entanglement and quantum information processing in cavity QED. Phys Rev Lett 2000;85:2392–5.
[98] Imamog A, Awschalom DD, Burkard G, et al. Quantum information processing using quantum dot spins and cavity QED. Phys Rev Lett 1999;83:4204.
[99] Gong Y, Vučković J. Design of plasmon cavities for solid-state cavity quantum electrodynamics applications. Appl Phys Lett 2007;90:033113.
[100] Hill MT, Oei YS, Smalbrugge B, et al. Lasing in metallic-coated nanocavities. Nat Photon 2007;1:589–94.
[101] Aune B, Bandelmann R, Bloess D, et al. Superconducting TESLA cavities. Phys Rev Spec Top Accelerat Beams 2000;3:092001.
[102] Chan S, Reid M, Ficek Z. Entanglement evolution of two remote and non-identical Jaynes-Cummings atoms. J Phys B Atom Mol Opt Phys 2009;42:065507.
[103] Khitrova G, Gibbs HM, Kira M, Koch SW, Scherer A. Vacuum Rabi splitting in semiconductors. Nat Phys 2006;2:81–90.
[104] Raimond J-M, Brune M, Haroche S. Manipulating quantum entanglement with atoms and photons in a cavity. Rev Mod Phys 2001;73:565.
[105] Peyronel T, Firstenberg O, Liang QY, et al. Quantum nonlinear optics with single photons enabled by strongly interacting atoms. Nature 2012;488:57–60.
[106] Wu FY, Ezekiel S, Ducloy M, Mollow BR. Observation of amplification in a strongly driven two-level atomic system at optical frequencies. Phys Rev Lett 1977;38:1077–80.
[107] Agarwal GS. Vacuum-field Rabi splittings in microwave absorption by Rydberg atoms in a cavity. Phys Rev Lett 1984;53:1732–4.
[108] Fink JM, Göppl M, Baur M, et al. Climbing the Jaynes-Cummings ladder and observing its nonlinearity in a cavity QED system. Nature 2008;454:315–8.
[109] Johansson J, Saito S, Meno T, et al. Vacuum Rabi oscillations in a macroscopic superconducting qubit LC oscillator system. Phys Rev Lett 2006;96:127006.
[110] Hutchison JA, Schwartz T, Genet C, et al. Modifying chemical landscapes by coupling to vacuum fields. Angew Chem Int Ed Engl 2012;51:1592–6.
[111] Fontcuberta i Morral A, Stellacci F. Light-matter interactions: ultrastrong routes to new chemistry. Nat Mater 2012;11:272–3.
[112] Galego J, Garcia-Vidal FJ, Feist J. Cavity-induced modifications of molecular structure in the strong-coupling regime. Phys Rev X 2015;5:041022.
[113] Schwartz T, Hutchison JA, Léonard J, Genet C, Haacke S, Ebbesen TW. Polariton dynamics under strong light-molecule coupling. ChemPhysChem 2013;14:125–31.
[114] Janietz S, Bradley DDC, Grell M, Giebeler C, Inbasekaran M, Woo, EP. Electrochemical determination of the ionization potential and electron affinity of poly(9,9-dioctylfluorene). Appl Phys Lett 1998;73:2453–5.
[115] Miroshnichenko AE, Flach S, Kivshar YS. Fano resonances in nanoscale structures. Rev Mod Phys 2010;82:2257.
[116] Shannon CE. Communication theory of secrecy systems. Bell Labs Tech J 1949;28:656–715.
[117] Pellizzari T, Gardiner SA, Cirac JI, Zoller P. Decoherence, continuous observation, and quantum computing: a cavity QED model. Phys Rev Lett 1995;75:3788–91.
[118] Turchette QA, Hood CJ, Lange W, Mabuchi HJKH, Kimble HJ. Measurement of conditional phase-shifts for quantum logic. Phys Rev Lett 1995;75:4710–3.
[119] Gershenfeld NA, Chuang IL. Bulk spin-resonance quantum computation. Science 1997;275:350–6.
[120] Jones JA, Mosca M, Hansen RH. Implementation of a quantum search algorithm on a quantum computer. Nature 1998;393:344–6.
[121] Steane A. The ion trap quantum information processor. Appl Phys B Lasers Opt 1997;64:623–42.
[122] Cirac JI, Zoller P. Quantum computations with cold trapped ions. Phys Rev Lett 1995;74:4091–4.
[123] Monroe C. Quantum information processing with atoms and photons. Nature 2002;416:238–46.
[124] Osnaghi S, Bertet P, Auffeves A, et al. Coherent control of an atomic collision in a cavity. Phys Rev Lett 2001;87:037902.
[125] Bennett CH, DiVincenzo DP. Quantum information and computation. Nature 2000;404:247–55.
[126] Nielsen MA, Chuang I. Quantum computation and quantum information. AAPT, 2002;70:558–9.
[127] Pelton M, Yamamoto Y. Ultralow threshold laser using a single quantum dot and a microsphere cavity. Phys Rev A 1999;59:2418.
[128] Alfano RR. The supercontinuum laser source, New York: Springer 1989.
[129] Kelly KL, Coronado E, Zhao LL, Schatz GC. The optical properties of metal nanoparticles: the influence of size, shape, and dielectric environment. J Phys Chem B, 2003;107:668–77.
[130] Nye J, Hajnal J. The wave structure of monochromatic electromagnetic radiation. Proc R Soc Lond A Math Phys Eng Sci 1987;409:21–36.
[131] Björk G, Machida S, Yamamoto Y, Igeta K. Modification of spontaneous emission rate in planar dielectric microcavity structures. Phys Rev A 1991;44:669–81.
[132] Yamamoto Y, Machida S, Björk G. Microcavity semiconductor laser with enhanced spontaneous emission. Phys Rev A 1991;44:657–68.
[133] Noda S, Fujita M, Asano T. Spontaneous-emission control by photonic crystals and nanocavities. Nat Photon 2007;1:449–58.
[134] Knoll W. Interfaces and thin films as seen by bound electromagnetic waves. Annu Rev Phys Chem 1998;49:569–638.

[135] Zhang S, Bao K, Halas NJ, Xu H, Nordlander P. Substrate-induced Fano resonances of a plasmonic nanocube: a route to increased-sensitivity localized surface plasmon resonance sensors revealed. Nano Lett 2011;11:1657–63.
[136] Moskovits M. Surface-enhanced Raman spectroscopy: a brief retrospective. J Raman Spectrosc 2005;36:485–96.
[137] Ergin T, Stenger N, Brenner P, Pendry JB, Wegener M. Three-dimensional invisibility cloak at optical wavelengths. Science 2010;328:337–9.
[138] Lal S, Clare SE, Halas NJ. Nanoshell-enabled photothermal cancer therapy: impending clinical impact. Acc Chem Res 2008;41:1842–51.
[139] Brongersma ML, Halas NJ, Nordlander P. Plasmon-induced hot carrier science and technology. Nat Nanotechnol 2015;10:25–34.
[140] Mubeen S, Lee J, Singh N, Krämer S, Stucky GD, Moskovits M. An autonomous photosynthetic device in which all charge carriers derive from surface plasmons. Nat Nanotechnol 2013;8:247–51.
[141] Ding Q, Shi Y, Chen M, et al. Ultrafast dynamics of plasmon-exciton interaction of Ag nanowire-graphene hybrids for surface catalytic reactions. Sci Rep 2016;6:32724.
[142] Fleischmann M, Hendra PJ, McQuillan AJ. Raman spectra of pyridine adsorbed at a silver electrode. Chem Phys Lett 1974;26:163–6.
[143] Campion A, Kambhampati P. Surface-enhanced Raman scattering. Chem Soc Rev 1998;27:241–50.
[144] Yeh D-M, Shi Y, Chen M. Localized surface plasmon-induced emission enhancement of a green light-emitting diode. Nanotechnology 2008;19:345201.
[145] Schaadt DM, Feng B, Yu ET. Enhanced semiconductor optical absorption via surface plasmon excitation in metal nanoparticles. Appl Phys Lett 2005;86:063106.
[146] Govorov AO, Bryant GW, Zhang W, et al. Exciton-plasmon interaction and hybrid excitons in semiconductor-metal nanoparticle assemblies. Nano Lett 2006;6:984–94.
[147] Drexhage KH. IV interaction of light with monomolecular dye layers. Prog Opt 1974;12:163–232.
[148] Berman P. Analysis of dynamical suppression of spontaneous emission. Phys Rev A 1998;58:4886.
[149] Yang KY, Choi KC, Ahn CW. Surface plasmon-enhanced spontaneous emission rate in an organic light-emitting device structure: cathode structure for plasmonic application. Appl Phys Lett 2009;94:121.
[150] Pelton M. Modified spontaneous emission in nanophotonic structures. Nat Photon 2015;9:427–35.
[151] Tignon J, Bryant GW, Zhang W, et al. From Fermi's golden rule to the vacuum Rabi splitting: magnetopolaritons in a semiconductor optical microcavity. Phys Rev Lett 1995;74:3967.
[152] Barnes W. Fluorescence near interfaces: the role of photonic mode density. J Mod Opt 1998;45:661–99.
[153] Kuhn H. Classical aspects of energy transfer in molecular systems. J Chem Phys 1970;53:101–8.
[154] Giannini V, Fernández-Domínguez AI, Heck SC, Maier SA. Plasmonic nanoantennas: fundamentals and their use in controlling the radiative properties of nanoemitters. Chem Rev 2011;111:3888–912.
[155] Choi H, Pile DF, Nam S, Bartal G, Zhang X. Compressing surface plasmons for nano-scale optical focusing. Opt Express 2009;17:7519–24.
[156] Aubry A, Lei DY, Fernández-Domínguez AI, Sonnefraud Y, Maier SA, Pendry JB. Plasmonic light-harvesting devices over the whole visible spectrum. Nano Lett 2010;10:2574–9.
[157] Xia H-R, Ye C-Y, Zhu S-Y. Experimental observation of spontaneous emission cancellation. Phys Rev Lett 1996;77:1032.
[158] Rikken G, Kessener Y. Local field effects and electric and magnetic dipole transitions in dielectrics. Phys Rev Lett 1995;74:880–3.
[159] Tam F, Goodrich GP, Johnson BR, Halas NJ. Plasmonic enhancement of molecular fluorescence. Nano Lett 2007;7:496–501.
[160] Aroca R. Surface-enhanced vibrational spectroscopy. Chichester, West Sussex, England: John Wiley & Sons, 2006.
[161] Xu H, Bjerneld EJ, Käll M, Börjesson L. Spectroscopy of single hemoglobin molecules by surface enhanced Raman scattering. Phys Rev Lett 1999;83:4357.
[162] Le Ru E, Etchegoin P. Principles of surface-enhanced Raman spectroscopy and related plasmonic effects. Oxford, UK: Elsevier, 2008.
[163] Le Ru E, Blackie E, Meyer M, Etchegoin PG. Surface enhanced Raman scattering enhancement factors: a comprehensive study. J Phys Chem C 2007;111:13794–803.
[164] Osawa M, Matsuda N, Yoshii K, Uchida I. Charge transfer resonance Raman process in surface-enhanced Raman scattering from p-aminothiophenol adsorbed on silver: Herzberg-Teller contribution. J Phys Chem 1994;98:12702–7.
[165] Rao AM, Eklund PC, Bandow S, Thess A, Smalley RE. Evidence for charge transfer in doped carbon nanotube bundles from Raman scattering. Nature 1997;388:257–9.
[166] Kang L, Chu J, Zhao H, Xu P, Sun M. Recent progress in the applications of graphene in surface-enhanced Raman scattering and plasmon-induced catalytic reactions. J Mater Chem C 2015;3:9024–37.
[167] Fang Y, Sun M. Nanoplasmonic waveguides: towards applications in integrated nanophotonic circuits. Light Sci Appl 2015;4:e294.
[168] Novotny L, Hecht B. Principles of nano-optics. NY, USA: Cambridge University Press, 2012.
[169] Nie S, Emory SR. Probing single molecules and single nanoparticles by surface-enhanced Raman scattering. Science 1997;275:1102–6.
[170] Kneipp K, Wang Y, Kneipp H, et al. Single molecule detection using surface-enhanced Raman scattering (SERS). Phys Rev Lett 1997;78:1667.
[171] Ambrose WP, Goodwin PM, Martin JC, Keller RA. Single molecule detection and photochemistry on a surface using near-field optical excitation. Phys Rev Lett 1994;72:160–3.
[172] Kang Y, Najmaei S, Liu Z, et al. Plasmonic hot electron induced structural phase transition in a MoS_2 monolayer. Adv Mater 2014;26:6467–71.
[173] Masuda H, Fukuda K. Ordered metal nanohole arrays made by a two-step replication of honeycomb structures of anodic alumina. Science 1995;268:1466–8.
[174] Michaels AM, Jiang J, Brus L. Ag nanocrystal junctions as the site for surface-enhanced Raman scattering of single rhodamine 6G molecules. J Phys Chem B 2000;104:11965–71.
[175] Michaels AM, Nirmal M, Brus L. Surface enhanced Raman spectroscopy of individual rhodamine 6G molecules on large Ag nanocrystals. J Am Chem Soc 1999;121:9932–9.
[176] Li JF, Huang YF, Ding Y, et al. Shell-isolated nanoparticle-enhanced Raman spectroscopy. Nature 2010;464:392–5.

[177] Lakowicz JR, Geddes CD, Gryczynski I, et al. Advances in surface-enhanced fluorescence. Biomed Opt 2004;2004:10–28.
[178] Liebermann T, Knoll W. Surface-plasmon field-enhanced fluorescence spectroscopy. Colloids Surf A Physicochem Eng Aspects 2000;171:115–30.
[179] Aslan K, Gryczynski I, Malicka J, Matveeva E, Lakowicz JR, Geddes CD. Metal-enhanced fluorescence: an emerging tool in biotechnology. Curr Opin Biotechnol 2005;16:55–62.
[180] Sokolov K, Chumanov G, Cotton TM. Enhancement of molecular fluorescence near the surface of colloidal metal films. Anal Chem 1998;70:3898–905.
[181] Käll M, Xu H, Johansson P. Field enhancement and molecular response in surface-enhanced Raman scattering and fluorescence spectroscopy. J Raman Spectrosc 2005;36:510–4.
[182] Zhang J, Fu Y, Chowdhury MH, Lakowicz JR. Metal-enhanced single-molecule fluorescence on silver particle monomer and dimer: coupling effect between metal particles. Nano Lett 2007;7:2101–7.
[183] Martorell J, Lawandy N. Observation of inhibited spontaneous emission in a periodic dielectric structure. Phys Rev Lett 1990;65:1877–80.
[184] Park JH, Lim YT, Park OO, Kim JK, Yu J-W, Kim YC. Polymer/gold nanoparticle nanocomposite light-emitting diodes: enhancement of electroluminescence stability and quantum efficiency of blue-light-emitting polymers. Chem Mater 2004;16:688–92.
[185] Anger P, Bharadwaj P, Novotny L. Enhancement and quenching of single-molecule fluorescence. Phys Rev Lett 2006;96:113002.
[186] Yang X, Yua H, Guo X, et al. Plasmon-exciton coupling of monolayer MoS_2-Ag nanoparticles hybrids for surface catalytic reaction. Mater Today Energy 2017;5:72–8.
[187] Kawata S, Inouye Y, Verma P. Plasmonics for near-field nano-imaging and superlensing. Nat Photon 2009;3:388–94.
[188] Lakowicz JR. Radiative decay engineering 5: metal-enhanced fluorescence and plasmon emission. Anal Biochem 2005;337:171–94.
[189] Song J-H, Atay T, Shi S, Urabe H, Nurmikko AV. Large enhancement of fluorescence efficiency from CdSe/ZnS quantum dots induced by resonant coupling to spatially controlled surface plasmons. Nano Lett 2005;5:1557–61.
[190] Lippincott-Schwartz J, Patterson GH. Photoactivatable fluorescent proteins for diffraction-limited and super-resolution imaging. Trends Cell Biol 2009;19:555–65.
[191] Li G, Shrotriya1 V, Huang J, et al. High-efficiency solution processable polymer photovoltaic cells by self-organization of polymer blends. Nat Mater 2005;4:864–8.
[192] Carlson DE, Wronski CR. Amorphous silicon solar cell. Appl Phys Lett 1976;28:671–3.
[193] Garnett E, Yang P. Light trapping in silicon nanowire solar cells. Nano Lett 2010;10:1082–7.
[194] Garnett EC, Yang P. Silicon nanowire radial p-n junction solar cells. J Am Chem Soc 2008;130:9224–5.
[195] Atwater HA, Polman A. Plasmonics for improved photovoltaic devices. Nat Mater 2010;9:205–13.
[196] Hains AW, Liang Z, Woodhouse MA, Gregg BA. Molecular semiconductors in organic photovoltaic cells. Chem Rev 2010;110:6689–735.
[197] Ito K, Nakazawa T. Electrical and optical properties of stannite-type quaternary semiconductor thin films. Jpn J Appl Phys 1988;27:2094.
[198] Ferry VE, Munday JN, Atwater HA. Design considerations for plasmonic photovoltaics. Adv Mater 2010;22:4794–808.
[199] Pankove JI. Optical processes in semiconductors. Mineola, NY, USA: Dover Publications, 1971.
[200] Munday JN, Atwater HA. Large integrated absorption enhancement in plasmonic solar cells by combining metallic gratings and antireflection coatings. Nano Lett 2010;11:2195–201.
[201] Catchpole K, Polman A. Design principles for particle plasmon enhanced solar cells. Appl Phys Lett 2008;93:191113.
[202] Nakayama K, Tanabe K, Atwater HA. Plasmonic nanoparticle enhanced light absorption in GaAs solar cells. Appl Phys Lett 2008;93:121904.
[203] Brown MD, Suteewong T, Kumar RS, et al. Plasmonic dye-sensitized solar cells using core-shell metal-insulator nanoparticles. Nano Lett 2010;11:438–45.
[204] Standridge SD, Schatz GC, Hupp JT. Distance dependence of plasmon-enhanced photocurrent in dye-sensitized solar cells. J Am Chem Soc 2009;131:8407–9.
[205] Jeong NC, Prasittichai C, Hupp JT. Photocurrent enhancement by surface plasmon resonance of silver nanoparticles in highly porous dye-sensitized solar cells. Langmuir 2011;27:14609–14.
[206] Novotny L, Van Hulst N. Antennas for light. Nat Photon 2011;5:83–90.
[207] Lal S, Link S, Halas NJ. Nano-optics from sensing to waveguiding. Nat Photon 2007;1:641–8.